Proceedings World Geothermal Congress 2020+1
Reykjavik, Iceland, April - October 2021

Application of a Detailed and Comprehensive Computational Chemical Geothermometer to Low Enthalpy Geothermal Waters in Northern Greece

Apostolos Arvanitis, Maria Papachristou and George Verros

Hellenic Survey of Geology and Mineral Exploration (H.S.G.M.E.), 1 Sp. Louis str., 13677, Acharnae, Greece

Department of Geology, Aristotle University of Thessaloniki, GR-54124, Thessaloniki, Greece

Department of Chemistry, Aristotle University of Thessaloniki, GR-54124, Thessaloniki, Greece

arvanitis@igme.gr, mariap@geo.auth.gr, gdverros@gmail.com

Keywords: geothermometry, geochemistry, chemical equilibrium, minerals, low enthalpy waters, reservoir temperature, Greece

ABSTRACT

Various chemical geothermometers are used to estimate deep geothermal reservoir temperatures based on the chemical composition of hot waters as a function of the concentration of specific elements and constituents (Na, K, Ca, Mg, Li and SiO_2). Nevertheless, the application of various geothermometers often results in large deviations of the estimated reservoir temperature. A new detailed and Comprehensive Computational Chemical Geothermometry (CCG) method is proposed in this paper. This novel methodology is based on the consideration of the equilibrium between geothermal water and specific minerals at a given temperature within deeper reservoir. It consists of two stages: (a) Initially, specific minerals are assumed to be in equilibrium with the reservoir fluid based on a detailed chemical analysis of the geothermal fluid (selection of minerals) (b) In a second stage, an optimization technique is applied to estimate the optimal temperature for the water in the reservoir by minimizing the deviation from equilibrium. This paper describes and discusses the application of the Comprehensive Computational Chemical Geothermometer (CCG) to geothermal waters from significant low enthalpy geothermal fields in Northern Greece, i.e. Therma-Nigrita, Akropotamos, Eratino-Chrysoupolis, Neo Erasmio-Magana, Aristino-Alexandroupolis. These fields are of high interest for further development and investments. The obtained results are compared with the ones from other 'classic' geothermometers, whereas the validity and reliability of the proposed CCG methodology are evaluated.

1. INTRODUCTION

Chemical geothermometers constitute a useful tool for estimating deep geothermal reservoir temperatures based on the chemical composition of hot waters from spring and wells. The reservoir temperature is determined as a function of the concentration of specific elements and constituents.

Chemical geothermometers can be classified into the following main groups:

- Silica geothermometers (SiO_2 solubility), based on the equilibrium of the SiO_2-H_2O system (Giggenbach et al., 1983)
- Alkali geothermometers (or Cation geothermometers) Na-K, Na-K-Ca, Na-K-Ca-Mg, Na-K-Mg, Na-Li, Li-Mg, K-Mg, Na-Ca, K-Ca, based on the ratios between alkali elements (Arnórsson et al, 1983; Fournier and Truesdell, 1973; Fournier et al, 1974; Fournier, 1977; Fournier, 1979; Fournier and Potter, 1979)
- Empirical geothermometers (Giampaolo et al, 1992) and Graphical methods (Spycher et al., 2014).

There are large deviations in the estimated reservoir temperatures using existing literature geothermometers. A novel method for estimating reservoir temperature is proposed: the detailed and Comprehensive Computational Chemical Geothermometer (CCG). This computational methodology could be viewed as an alternatively methodology to the graphs proposed by Pang and Reed (1998) for the estimation of reservoir candidate minerals and temperature. This new approach has been applied to geothermal waters from significant low enthalpy geothermal fields in Northern Greece, i.e. Therma-Nigrita, Akropotamos, Eratino-Chrysoupolis, Neo Erasmio-Magana, Aristino-Alexandroupolis. These fields are of high interest for further development and exploitation. The obtained results are compared with the ones from other classic geothermometers and the validity and reliability of the proposed CCG methodology are evaluated.

2. THE COMPREHENSIVE COMPUTATIONAL CHEMICAL GEOTHERMOMETER (CCG)

2.1 Basic Assumptions

The development of the detailed and Comprehensive Computational Chemical Geothermometry (CCG) has been based on the consideration of the equilibrium between the geothermal waters and specific minerals at a given temperature within the geothermal reservoir. Basic assumptions used in the CCG methodology are as follows (Verros et al., 2007; Verros and Papachristou, 2014):

- Temperature-dependent reactions occur at depth.
- All constituents involved in a temperature-dependent reaction are sufficiently abundant.
- Water-rock equilibrium occurs at the reservoir temperature.
- Little or no-equilibration occurs or change in composition occurs at lower temperatures as the water flows from the reservoir to the surface.
- The hot water coming from deep in the system does not mix with cooler shallow groundwater.
- Equilibrium can be established at a certain temperature and depth between one or more minerals and the geothermal fluid.

2.2 Theoretical Issues

The Comprehensive Computational Chemical Geothermometry (CCG) combines temperature-dependent reactions that occur at depth, and water-rock equilibrium. The attainment of equilibrium inside the reservoir depends on a number of factors, such as: (i) the kinetics of the particular reaction, (ii) the reservoir temperature, (iii) the reactivity of rock wall, (iv) the concentrations of the indicator elements in the water and (v) the residence time of the water in the reservoir at the particular temperature. Consequently, equilibrium in the reservoir may be attained for some reactions but not for others (Verros et al., 2007).

Table 1 summarizes various chemical reactions between dissolved species in the geothermal fluid (Verros et al., 2007; Verros and Parachristou, 2017). Equilibrium is assumed for chemical reactions between dissolved species. The equilibrium can be established at a certain temperature and depth between mineral(s) and geothermal fluids according to general form:

$$Ax+By+Nz = xA+yB+zN \tag{1}$$

where A and B are H, Na, K, Ca, Mg, Al and N is an anion. Equilibrium reactions between minerals and the dissolved species are presented in Table 2. Each mineral is associated with an equilibrium reaction, which is characterized by the solubility product K_{sp} and an equilibrium constant K_{oj}.

Table 1: Equilibrium reactions in the geothermal fluid

Chemical Reaction	Chemical Reaction	Chemical Reaction
$H_2O = H^+ + OH^-$	$H_2CO_3 = H^+ + HCO_3^-$	$HCO_3^- = H^+ + CO_3^-$
$H_2SO_4 = H^+ + HSO_4^-$	$HSO_4^- = H^+ + SO_4^{-2}$	$H_4SiO_4 = H^+ + H_3SiO_4^-$
$CaOH^+ = Ca^{+2} + OH^-$	$MgOH^+ = Mg^{+2} + OH^-$	$H_3SiO_4^- = H^+ + H_2SiO_4^{-2}$
$CaSO_4 = Ca^{+2} + SO_4^{-2}$	$MgSO_4 = Mg^{+2} + SO_4^{-2}$	$NaH_3SiO_4 = Na^+ + H_3SiO_4^-$
$CaHCO_3^+ = Ca^{+2} + HCO_3^-$	$MgHCO_3^+ = Mg^{+2} + HCO_3^-$	$NaCl = Na^+ + Cl^-$
$KCl = K^+ + Cl^-$	$MgCO_3 = Mg^{+2} + CO_3^{-2}$	$NaSO_4^- = Na^+ + SO_4^{-2}$
$KSO_4^- = K^+ + SO_4^{-2}$	$Al(SO_4)_2^- = Al(SO_4)^+ + SO_4^{-2}$	$Al(OH)_3 = Al(OH)_2^+ + OH^-$
$Al(OH)_4^- = Al(OH)_3 + OH^-$	$Al(SO_4)^+ = Al^{+3} + SO_4^{-2}$	$AlOH^{+2} = Al^{+3} + OH^-$
$Al(OH)_2^+ = AlOH^{+2} + OH^-$		

Table 2: Equilibrium reactions between minerals and dissolved species

Mineral (Chemical Formula)	Reaction
ADULARIA ($KAlSi_3O_8$)	$KAlSi_3O_8 + 8H_2O = K^+ + Al(OH)_4^- + 3H_4SiO_4$
LOW ALBITE ($NaAlSi_3O_8$)	$NaAlSi_3O_8 + 8H_2O = Na^+ + Al(OH)_4^- + 3H_4SiO_4$
ANALCIME ($NaAlSi_3O_8.H_2O$)	$NaAlSi_3O_8.H_2O + 5H_2O = Na^+ + Al(OH)_4^- + 2H_4SiO_4$
CALCITE ($CaSO_4$)	$CaSO_4 = Ca^{+2} + SO_4^{-2}$
CHALKEDONY (SiO_2)	$SiO_2 + 2H_2O = H_4SiO_4$
Mg-CHLORITE ($Mg_5Al_2Si_3O_{10}(OH)_8$)	$Mg_5Al_2Si_3O_{10}(OH)_8 + 10H_2O = 5Mg^{+2} + Al(OH)_4^- + H_4SiO_4 + 8OH^-$
LAUMONTITE ($CaAl_2Si_4O_{12}.4H_2O$)	$CaAl_2Si_4O_{12}.4H_2O + 8H_2O = Ca^{+2} + 4Al(OH)_4^- + 4H_4SiO_4$
MICROCLINE ($KAlSi_3O_8$)	$KAlSi_3O_8 + 8H_2O = K^+ + Al(OH)_4^- + 3H_4SiO_4$
Ca-MONTMOR($Ca_{0.167}Al_{2.33}Si_4O_{3.67}O_{10}(O)_2$)	$6Ca_{0.167}Al_{2.33}Si_4O_{3.67}O_{10}(OH)_2 + 60H_2O + 12OH^- = Ca^{*2} + 14Al(OH)_4^- + 22H_4SiO_4$
K-MONTMOR($K_{0.33}Al_{2.33}Si_4O_{3.67}O_{10}(OH)_2$)	$3K_{0.33}Al_{2.33}Si_4O_{3.67}O_{10}(OH)_2 + 30H_2O + 6OH^- = K^+ + 7Al(OH)_4^- + 11H_4SiO_4$
MgMONTMOR($Mg_{0.167}Al_{2.33}Si_4O_{3.67}O_{10}(OH)_2$)	$6Mg_{0.167}Al_{2.33}Si_4O_{3.67}O_{10}(OH)_2 + 60H_2O + 12OH^- = Mg^{+2} + 14Al(OH)_4 + 22H_4SiO_4$
Na-MONTMOR($Na_{0.33}Al_{2.33}Si_4O_{3.67}O_{10}(OH)_2$)	$3Na_{0.33}Al_{2.33}Si_4O_{3.67}O_{10}(OH)_2 + 30H_2O + 6OH^- = Na^+ + 7Al(OH)_4^- + 11H_4SiO_4$
MUSCOVITE($Kal_3Si_3O_{10}(OH)_2$)	$Kal_3Si_3O_{10}(OH)_2 + 10H_2O + OH^- = K^+ + 3Al(OH)_4^- + 3H_4SiO_4$
PREHNITE($Ca_2Al_2Si_3O_{10}(OH)_2$)	$Ca_2Al_2Si_3O_{10}(OH)_2 + 10H_2O = 2Ca^{+2} + 2Al(OH)_4^- + 3H_4SiO_4 + 2OH^-$
QUARTZ(SiO_2)	$SiO_2 + 2H_2O = H_4SiO_4$
WALRAKITE($CaAl_2Si_4O_{12}.2H_2O$)	$CaAl_2Si_4O_{12}.2H_2O + 10H_2O = Ca^{+2} + 2Al(OH)_4^- + 4H_4SiO_4$
WOLLASTONITE ($CaSiO_3$)	$CaSiO_3 + 2H^+ + H_2O = Ca^{+2} + 14Al(OH)_4^- + H_4SiO_4$
ZOISITE($Ca_2Al_2Si_3O_{12}(OH)_2$)	$Ca_2Al_2Si_3O_{12}(OH)_2 + 8H_2O = 2Ca^{+2} + 3Al(OH)_4^- + 3H_4SiO_4 + OH^-$

The equilibrium for each j-th mineral is characterized by the solubility product $K_{sp,j}$ (Verros and Papachristou, 2017):

$$K_{sp,j} = \frac{\prod_i m_i^{\nu_{Oi}} \gamma_i^{\nu_{Oi}}}{a_{Oi}} \tag{2}$$

where ν_{Oi}, m_i, γ_i and a_{Oi} are the number of the component species in one mole of the dissolved species, molality (number of moles of solute/substance per kilogram), activity coefficient (ratio of chemical activity of any substance to its molar concentration), activity (a measure of the effectiveness concentration of a species in a mixture), respectively. In this equation, ν_{Oi} is negative for components on the left hand side of the reaction and symbol **Π** presents product. In the present discussion, $a_{Oi}=1$ because mineral solid solutions are excluded (Verros et al., 2007). The activity coefficients γ_i are calculated as a function of temperature and species concentration by using standard methods (Parkhurst, 1990). The solubility product constant $K_{sp,j}$ is a function of temperature.

The equilibrium constant K_{oj} for a reaction having a general form such as Ax+By+Nz = xA+yB+zN, where A and B are H, Na, K, Ca, Mg, Al and N is an anion, can be defined as:

$$K_{oj} = [A]^x[B]^y[N]^z \tag{3}$$

The values of equilibrium constant K_{oj} as a function of temperature for various minerals are given in Table 3. In the equilibrium case, the solubility product $K_{sp,j}$ is identical to the equilibrium constant K_{oj}.

Table 3: Equilibrium constants for the disproportionation of selected geothermal minerals (Arnórsson et al, 1982; Reed, 1982; Tole et al, 1993)

	Mineral	Chemical Reaction	Log$_{10}$ K
1	Adularia	$KAlSi_3O_8 + 8H_2O = K^+ + Al(OH)_4^- + 3H_4SiO_4^o$	$38.85-0.0458T-17260/T+1012722/T^2$
2	Low albite	$NaAlSi_3O_8 + 8H_2O = Na^+ + Al(OH)_4^- + 3H_4SiO_4^o$	$36.83-0.0439T-16474/T+1004631/T^2$
3	Analcime	$NaAlSi_3O_8.H_2O + 5H_2O = Na^+ + Al(OH)_4^- + 2H_4SiO_4^o$	$34.08-0.0407T-14577/T+970981/T^2$
4	Anhydrite	$CaSO_4 = Ca^{2+} + SO_4^{2-}$	$6.2-0.0229T-1217/T$
5	Calcite	$CaCO_3 = Ca^{2+} + CO_3^{2-}$	$10.22-0.0349T-2476/T$
6	Chalkedony	$SiO_2 + 2H_2O = H_4SiO_4^o$	$0.11-1101/T$
7	Mg-Chlorite	$Mg_5Al_2Si_3O_{10}(OH)_8+10H_2O =5Mg^{2+} + Al(OH)_4^- + H_4SiO_4^o + 8OH^-$	$-1022.12-0.3861T+9363/T+412.46\text{Log }T$
8	Laumontite	$CaAl_2Si_4O_{12}.4H_2O + 8H_2O = Ca^{+2} + 4Al(OH)_4^- + 4H_4SiO_4^o$	$65.95-0.0828T-28358/T+1916098/T^2$
9	Microcline	$KAlSi_3O_8 + 8H_2O = K^+ + Al(OH)_4^- + 3H_4SiO_4^o$	$44.55-0.0498T-19883/T+1214019/T^2$
10	Ca-Monimor	$6Ca_{0.167}Al_{2.33}Si_4O_{3.67}O_{10}(OH)_2 +60H_2O + 12OH^- = Ca^{2+} + 14Al(OH)_4^- + 22H_4SiO_4^o$	$30499.49+3.5109T-1954295/T+125536640/T^2 -10715.66\text{LogT}$
11	K-Monimor	$3K_{0.33}Al_{2.33}Si_4O_{3.67}O_{10}(OH)_2 +30H_2O + 6OH^- = K^+ + 7Al(OH)_4^- + 11H_4SiO_4^o$	$15075.11+1.7346T-967127/T+61985927/T^2-5294.721\text{LogT}$
12	Mg-Monimor	$6Mg_{0.167}Al_{2.33}Si_4O_{3.67}O_{10}(OH)_2 +60H_2O + 12OH^- = Mg^{2+} + 14Al(OH)_4^- + 22H_4SiO_4^o$	$30514.87+3.5188T-1953843/T+125538830/T^2-10723.71\text{LogT}$
13	Na-Monimor	$3Na_{0.33}Al_{2.33}Si_4O_{3.67}O_{10}(OH)_2 +30H_2O + 6OH^- = Na^+ + 7Al(OH)_4^- + 11H_4SiO_4^o$	$15273.90+1.7623T-978782/T+62805036/T^2-5366.188\text{LogT}$
14	Muscovite	$KAl_3Si_3O_{10} (OH)_2 + 10H_2O + OH^- = K^+ + 3Al(OH)_4^- + 3H_4SiO_4^o$	$6113.68+0.6914-394755/T+25226323/T^2-2144.77\text{LogT}$
15	Prehnite	$Ca_2Al_2Si_3O_{10} (OH)_2 + 10H_2O = 2Ca^{2+} + 2Al(OH)_4^- + 3H_4SiO_4^o + 2OH^-$	$90.53-0.1298T-36162/T + 2511432/T^2$
16	Quartz	$SiO_2 + 2H_2O = H_4SiO_4^o$	$0.41-1309/T$ (0-250^{0}C) $0.12 -1164/T$ (180-300^{0}C)
17	Walrakite	$CaAl_2Si_4O_{12} .2H_2O + 10H_2O = Ca^{2+} + 2Al(OH)_4^- + 4H_4SiO_4^o$	$61.-0.0847T-25018/T+1801911/T^2$
18	Wollastonite	$CaSiO3 + 2H^+ + H_2O = Ca^{2+} + 14Al(OH)_4^- + H_4SiO_4^o$	$-222.85-0.0337T+16258/T-671106/T^2+80.68\text{LogT}$
19	Zoisite	$Ca_2Al_2Si_3O_{12}(OH)_2 + 8H_2O = 2Ca^{+2} + 3Al(OH)_4^- + 3H_4SiO_4^o + OH^-$	$4467.61+5879T-169944/T - 1838.45\text{Log }T$

The characteristic ratio R_{kj} for the j-th mineral at each k-th temperature is the ratio between equilibrium constant K_{oj} and solubility product $K_{sp,j}$ and is estimated by the equation (Verros and Papachristou, 2017):

$$R_{kj} = \prod_{i} m_i^{v_{Oi}} \gamma_i^{v_{Oi}} \Big/ K_{sp,j} \tag{4}$$

In this equation: (a) γ_i are activity coefficients that are calculated as a function of temperature and species concentrations and set equal to unity based on standard methods, (b) $K_{sp,j}$ are solubility product constants, the values of which are a function of temperature for various minerals, and (c) m_i are molalities. The characteristic ratio R_{kj} is an indication of the presence of a selected mineral in the reservoir rocks at a given temperature. If the equilibrium assumption is satisfied, i.e. R_{kj}=1, for the j-th mineral at the the k-th temperature, then this mineral is selected as candidate mineral for the rock wall of the reservoir (Verros et al, 2007; Verros and Papachristou, 2014).

The molalities (m_i) are calculated by solving the respective mass balances. More specifically, one can directly relate the total mass M_i^t of the elements Na, K, Ca, Mg, Al, Cl, Si and the ions SO_4^{-2}, CO_3^{2-}, HCO_3^- to the various species concentration (see Table 1) by assuming equilibrium and by writing the respective mass balances. These non-linear algebraic mass balance equations are solved for a given temperature, by using standard numerical methods (Verros et al., 2007; Verros and Papachristou, 2014). The total mass M_i^t of each element to the various species concentrations is calculated by the equation (Reed, 1982):

$$\mathrm{M}_i^t = n_w \sum_k m_{ki} \tag{5}$$

where n_w refers to the mass of solvent water in kilograms. This parameter is directly obtained by the chemical analyses. For example, the above mass balance is written for the Na in the solution as (Verros et al., 2007):

$$\mathrm{M}^t{}_{N\alpha} = n_w \left[m_{Na} + m_{NaCl} + m_{NaSO_4} + m_{NaH_3SiO_4} \right] \tag{6}$$

The total mass of each element or ion is determined by chemical analysis (Verros and Papachristou, 2014).

Very often the total aluminum (Al) concentration is estimated with moderate accuracy, or, even worse, remains unknown. This is a serious problem, given that most of the minerals include Al (Tables 2 and 3) as a major component (Arnórsson et al., 1982; Reed, 1982; Tole et al., 1993). Moreover, the geothermal fluid is anticipated to be in equilibrium at least with two of the minerals that contain aluminum as a structural element (Pang and Reed, 1998). However, aluminum is sparingly soluble in water. The aluminum concentration can be measured or calculated as a function of geothermal fluid pH using sound physical chemistry principles or equations, such as (Hem and Roberson, 1967):

$$\log_{10}(C_{Al(OH)4}) = -pH + 14.2 \tag{7}$$

2.3 The Comprehensive Chemical Geothermometer (CCG) as a Two-Stage Methodology

The development of the CCG methodology and computed framework is based on the selection of minerals that might be in equilibrium with the water within the geothermal reservoir at a given temperature. SiO_2 contents and water temperature are essential data for the application of the CCG methodology. The selection of minerals is achieved by comparing, for a given temperature, the well established equilibrium constants of various minerals with the estimated values from water chemical analysis. An optimization technique is applied to estimate the optimal temperature for the water in the reservoir by minimizing the deviation from the equilibrium. Consequently, this methodology includes two stages (Verros et al., 2007; Verros and Papachristou, 2014; Verros and Papachristou, 2017):

- First stage: Selection of minerals that might be in equilibrium with the geothermal fluids in the reservoir based on a detail chemical analysis of the geothermal fluid.
- Second stage: Application of an optimization technique to estimate the optimal temperature for the water in the reservoir by minimizing the deviation from equilibrium.

2.3.1 First Stage of the CCG Methodology: Mineral Selection

The first stage deals with the selection of minerals which might be in equilibrium with the geothermal waters in the reservoir. At this stage (Verros et al., 2007; Verros and Papachristou, 2014; Verros and Papachristou, 2017):

1. Water chemical analysis is carried out and the concentrations of various constituents are determined (experimental section). The total mass of each element or ion is determined by chemical analysis.
2. Equilibrium is assumed for the chemical reactions between dissolved species in the geothermal fluid.
3. The total mass M_i^t of the elements Na, K, Ca, Mg, Al, Cl, Si and the ions SO_4^{-2}, CO_3^{2-}, HCO_3^- are related to the various species concentration (Table 1) by assuming an equilibrium and by solving the respective mass balances.
4. The non-linear mass balance equations are solved for a given temperature by using standard numerical methods.
5. The activity coefficients (γ_i) are set equal to unity by using standard methods (Parkhurst, 1990).
6. The values of the solubility product constants ($K_{sp,j}$) and equilibrium constants (K_{oj}) as a function of temperature for various minerals are given in standard references (Arnórsson et al., 1982; Reed, 1982; Tole, 1993).
7. It is assumed that there is equilibrium between geothermal fluid and specific minerals in the reservoir.
8. After calculating various species concentration, the characteristic ratio R_{kj} is estimated for the j-th mineral at each k-th temperature. The characteristic ratio R_{kj} is an indication of the presence of a selected mineral in the reservoir rocks at a given temperature.
9. If the equilibrium assumption is satisfied for the j-th mineral at the k-th temperature, i.e. R_{kj}=1, then this mineral is selected as a candidate mineral for the rock wall of the reservoir.
10. A number of candidate minerals are selected.
11. As a rule of thumb, the temperature of the spring, borehole or well is taken as a reference to select the candidate minerals.

2.3.2 Second Stage of the CCG Methodology: Optimization Technique and Estimation of Reservoir Temperature

The second stage deals with the estimation of temperature in the deeper geothermal reservoir using optimization techniques. The task is to estimate the optimal value of the reservoir temperature by selecting a proper objective function F in order to minimize the deviation of the characteristic ratio R_{kj}. For this purpose the material balances are solved for each k-th temperature and the R_{kj} values for the selected minerals are calculated. In each temperature value of the algorithm, the mass balances used to estimate the characteristic ratio R_{kj} have to be solved. This results in a two step optimization algorithm. The first step is the solution of mass balances and the next step is the estimation of reservoir temperature. Standard methods of non-linear optimization techniques are used to estimate the reservoir temperature by requiring the objective function F to be minimal (Verros and Papachristou, 2014).

The following form for the objective function F has been chosen (Verros and Papachristou, 2017):

$$F = \sum_{k=1}^{L}\sum_{j=1}^{N} w_{kj}\left(1 - R_{kj}\right)^2 \; j = 1,2,3 \tag{8}$$

In this equation, $w_{k,j}$ are the appropriate weights, N is the total number of minerals selected as candidate minerals for the reservoir rock at each temperature, k represents the different temperatures and j represents the different formulation of the objective function as different minerals are assumed to be in equilibrium with the geothermal fluid at various temperature as previous calculated. It was found convenient to set these weights $w_{k,j}$ equal to R_{kj}. The above form of the objective function F allows the application of different policies for candidate mineral selection. The first policy requires all candidate minerals (R_{kj} values close to 1) to participate in the objective function F and the other policy requires only the common candidate minerals in all tested temperatures to be included in the objective function. This results in an interval rather than in a single value of proposed reservoir temperatures.

The complete algorithm after the water chemical analysis and the selection of candidate minerals consists of the following steps (Verros and Papachristou, 2014):

1. An initial temperature is assumed.
2. The mass balances are solved for each element or ion in the geothermal fluid by using standards methods of numerical analysis.
3. The characteristic ratios R_{kj} are calculated for the specific minerals
4. The objective function F is calculated.
5. It is examined if the value of the objective function F is less than a given number or, in other words, if the convergence criteria are satisfied.
6. If the convergence criteria are satisfied then the algorithm is terminated. Otherwise, a new value for temperature is automatically assumed and the procedure of steps 2-5 is repeated.

In cases where mixing phenomena occur, the mixing ratio (V_2/V_1) is added in the optimizing procedure as an adjustable parameter along with the deep reservoir temperature. V_1 represents the volumetric flow from the main reservoir and V_2 is the volumetric flow of an additive such as sea water. A crucial assumption made is that the geothermal fluid acts as a buffer solution. This allows us to assume a constant pH of the geothermal fluid. It is also assumed that mixing with sea water has a limited effect on the temperature of geothermal fluid (Verros and Papachristou, 2017).

3. APPLICATION OF THE COMPREHENSIVE COMPUTATIONAL CHEMICAL GEOTHERMOMETER (CCG) TO GEOTHERMAL WATERS IN NORTHERN GREECE - COMPARISON WITH CLASSIC GEOTHERMOMETERS – EVALUATION OF THE RESULTS

The Comprehensive Computational Chemical Geothermometer (CCG) has been applied to geothermal waters from significant low enthalpy geothermal fields in Northern Greece (Macedonia and Thrace), The selected geothermal fields are as follows: Therma-Nigrita, Akropotamos, Eratino-Chrysoupolis, Neo Erasmio-Magana, Aristino-Alexandroupolis (Figure 1).

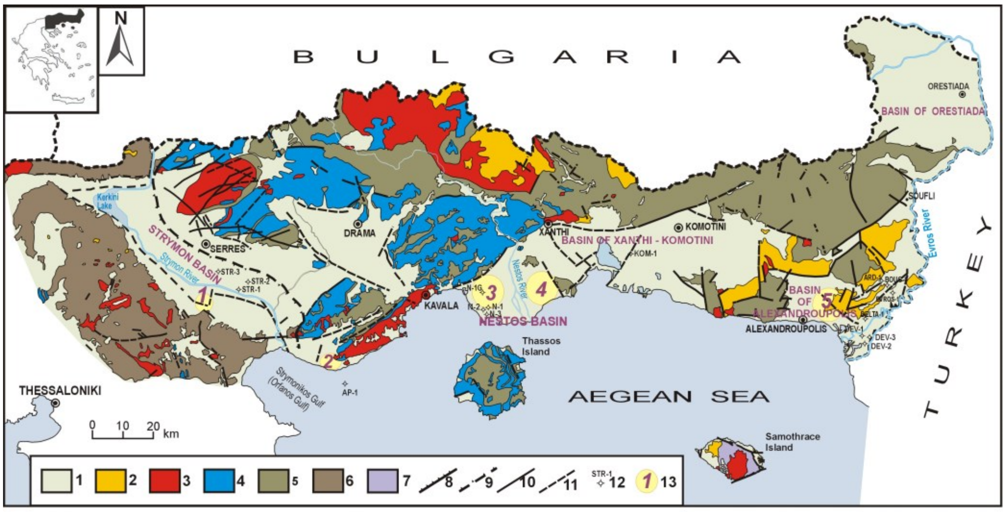

[1: Tertiary and Quaternary sediments, 2: Tertiary volcanic rocks, 3: Granites and granodiorites, 4: Marbles and limestones, 5: Metamorphosed rocks of Rhodope Massif, 6: Metamorphosed rocks of SMM Massif, 7: Low-grade metamorphosed rocks of Circum-Rhodope belt, 8: SMM & Rhodope probable contact, 10: Faults, 11: Probable faults, 12: Deep hydrocarbon exploration boreholes, 13: Low enthalpy geothermal fields *(the numeration of the fields is as follows: 1:Therma-Nigrita, 2 Akropotamos, 3: Eratino-Chrysoupolis, 4:Neo Erasmio - Magana 5: Aristino-Alexandroupolis)*]

Figure 1: Simplified geologic map of NE Greece with the locations of geothermal fields of Therma-Nigrita, Akropotamos, Eratino-Chrysoupolis, Neo Erasmio-Magana and Aristino-Alexandroupolis (Kolios et al, 2007).

These fields are of high interest for further development and investments. In all cases, it is assumed that the geothermal fluid is mixed with sea water. A crucial consideration that has been made is that the geothermal fluid acts as a buffer solution. It is also presumed that the pH of the geothermal fluid is constant and mixing with sea water has a very little effect on the temperature of the geothermal fluid. On the contrary, the mixing with even very small amounts of sea water has a profound effect on its chemical composition, leading not only to a variety of candidate minerals, but also to different estimates for the deep reservoir temperatures (Verros and Papachristou, 2017). The obtained results are compared to the ones from other classic geothermometers and the validity and reliability of the proposed CCG methodology are evaluated. The following literature geothermometers have been used for comparison:

(i) Silica geothermometers:
  - quartz - no steam loss, range 25-250°C, conductive cooling (Fournier, 1977)
  - chalcedony, range 0-250°C (Fournier, 1977)

(ii) Na/K geothermometer, range 25-250°C (Arnórsson et al., 1983)
(iii) Na/K geothermometer (Nieva and Nieva, 1987)
(iv) Na-K-Ca geothermometer (Fournier and Truesdell, 1983)
(v) Mg correction to Na-K-Ca geothermometer (Fournier and Potter, 1979)
(vi) Na-Li geothermometer (range 20-340°C), for Cl <0.3 mol/kg or around Cl<10,000 mg/l (Fouillac and Michard, 1981)
(vii) Na-Li geothermometer (Kharaka et al., 1982)
(viii) K-Mg geothermometer (Giggenbach, 1988)
(ix) Li-Mg geothermometer (Kharaka and Mariner, 1989).

3.1 Therma - Nigrita Geothermal Field (Strymon Basin, Macedonia)

The low enthalpy geothermal field of Therma-Nigrita is located in the SW part of the Strymon basin, which is a typical post-orogenic graben. The geothermal reservoir, with fluctuated thickness of 20 to 65m, is located at depths of 70-500m in the basal conglomerates and the fractured top the ophiolitic basement. It constitutes a confined aquifer containing geothermal waters of 40-64°C. Above the basal conglomerates, Neogene and Quaternary sediments, consisting of marls, sands and mainly clays, form an impervious cap for the geothermal fluids (Figure 2A). The upflow zone is located at the NW part of the field close to a NW-SE normal fault. Significant quantities of CO_2 are encountered (3.5-4.7 kg CO_2/t of geothermal water) and consequently, two-phase flow (H_2O+CO_2) occur at geothermal wells. The presence of CO_2, in combination with the temperature and the hydrostatic pressure, creates a constant artesian flow (Arvanitis et al., 1998; Karydakis et al; 2005).

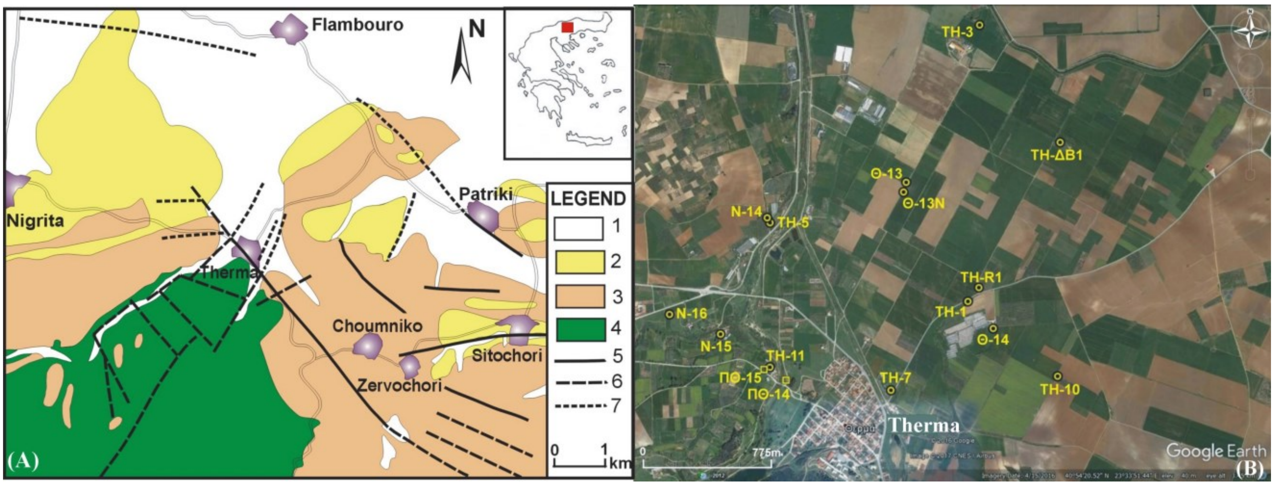

Figure 2: (A) Geological and tectonic setting of the Therma-Nigrita geothermal field [1. Sandy clays, sands, gravels, alluvial fans (Holocene), 2. Sands, gravels, clays and loams (Pleistocene), 3. Fine-layered silts, clays, sandy clays, lacustrine limestones, marls, marly limestones, silts, intercalations of gravels, sands, basal conglomerates (Neogene), 4. Ophiolites, 5. Faults, 6. Probable faults based on geophysical, geological and temperature data, 7. Probable faults by geophysical surveys] (Arvanitis et al., 1998), (B) The locations of wells and springs in the Therma-Nigrita geothermal field as depicted on the Google Earth Map.

Table A in Appendix summarizes the results of the chemical analyses of geothermal waters (Dimopoulos, 1990; Arvanitis et al., 1998; Karydakis et al., 1999; Athanassoulis et. al., 2009) collected from wells and springs indicated in Figure 2B along with fluid temperatures. The geothermal waters are mainly of Na-HCO_3 type, except the samples from wells TH-3 and TH-7 (Na,Ca-HCO_3 and Ca,Mg-HCO_3 types) and a few samples from well TH-11. They have TDS values 1.0-2.5 g/l and slightly acid character (pH<7). Geothermal waters form scales (mainly in the heat exchangers) and have corrosive character. They are classified as 'immature waters' according to the Giggenbach (1988) trilinear diagram. The deep reservoir temperature is estimated using both classic chemical geothermometers and the Comprehensive Computational Chemical Geothermometer (Table 4).

The Na/K and Na-K-Ca geothermometers yield high (overestimated) values. There are not applicable because the waters are acid 'immature', and rich in CO_2 and Ca^{2+}. Mg-correction for the Na-K-Ca geothermometers gives very low temperatures ($T \leq 60$°C, lower than exit temperature). The Na-Li geothermometer proposed by Kharaka et al. (1982) provides temperatures of 152-202.9°C, which are considered as overestimated. More realistic values (110-120°C) are calculated by the Na-Li geothermometer presented by Fouillac and Michard (1981) for Cl<0.3 mol/kg. The Na/Li geothermometer is sensitive to TDS and rock type and slight changes in Li concentrations during the ascent of fluid can affect the Na/Li ratio since Li is a minor constituent and Na is a major one (D'

Amore and Arnórsson, 2000). The Li-Mg geothermometer (Kharaka and Mariner, 1989) gives underestimated, unreliable and non-representative values (22-70.6°C). The K-Mg geothermometer (Giggenbach, 1988) yields slightly underestimated temperatures (49.7-106.9°C). Boiling does not occur. The geothermal waters contain dissolved CO_2, have low pH (generally $pH<7$) and are more reactive and therefore, they can easily pick up Mg from the peridotites in the upflow zones, thus increasing Mg concentrations. The chalcedony geothermometer (Fournier, 1977) is suitable for low temperature sources and gives temperatures of 55.9-108.4°C. The quartz geothermometer (no steam loss, conductive cooling) proposed by Fournier (1977) yields values ranging from 86.9 to 135.3°C**.** The geothermal waters are plotted on the Giggenbach and Coguel (1989) diagram (Powell and Cumming, 2010) and this plot shows that the probable deep temperatures vary between 90 and 110°C.

Table 4: Deep reservoir estimated temperatures at the Therma-Nigrita geothermal field using both classical chemical geothermometers and the Comprehensive Computational Chemical Geothermometer (CCG)

Water Samples	T(˚C)	SiO_2 quartz (i)	SiO_2 chalcedony (ii)	Na/K (iii)	Na/K (iv)	Na-K-Ca (v)	Na-K-Ca, Mg correction (vi)	Na-Li (vii)	Na-Li (viii)	K-Mg (ix)	Li-Mg (x)	CCG
TH-R1	59.8	123.8	95.7	305.3	290	239.9	34	104.9	173.0	105.7	66.5	**110-117**
TH-R1	60.9	122.1	93.9	304.9	290	240.7	35	106.7	174.5	106.9	68.0	**107-116**
TH-ΔB1	61.8	131.8	104.5	236.6	237	210.8	28	108.7	176,3	97.5	72.4	**119-125**
TH-ΔB1	61.7	132.4	105.2	232.4	234	209.1	28	107.1	174.9	97.2	72.5	**120-125**
TH-ΔB1	61.7	132.9	105.8	233.2	235	209.7	29	108.6	176.2	97.7	73.2	**120-125**
TH-1	59.0	118.9	90.4	244.6	244	210.5	20	139.8	202.9	91.3	76.2	**111**
TH-3	45.0	102.2	72.3	266.3	261	214.2	40	95.6	164.8	94.7	59.9	**93**
TH-5	42.0	107.0	77.5	257.5	254	215.9	19	98.2	167.1	91.9	60.0	**97**
TH-10	58.0	125.9	98.1	257.4	254	215.6	27	106.2	174.1	95.0	65.6	**97**
TH-7	48.0	86.9	55.9	336.8	314	53.4	53	123.1	188.7	49.7	22.0	**83**
TH-11	51.0	96.4	66.0	272.6	266	204.7	20	116.0	182.6	75.4	49.7	**92**
TH-11	42.4	121.2	92.9	240.4	240	202.8	18	118.4	184.7	83.4	62.7	**112**
TH-11	46.2	126.7	98.9	298.0	285	227.4	20	118.9	185.1	90.1	59.4	**110-120**
TH-11	46.0	124.8	96.9	279.3	271	220.6	20	81.7	152.3	89.4	48.5	**120**
TH-11	46.1	123.0	94.8	254.3	251	129.5	22	…	…	80.0	…	**118**
TH-11	47.6	…	…	237.4	238	142.2	32	…	…	87.6	…	**…**
TH-11	47.4	118.3	89.8	273.0	266	204.1	117	107.5	175.3	96.0	64.3	**113**
TH-11	48.0	126.8	99.0	274.4	267	217.9	49	111.4	178.6	96.7	66.0	**120**
TH-11	49.2	129.6	102.1	254.5	252	208.9	60	91.7	161.3	96.4	61.9	**122**
Θ-14	62.0	127.7	100.0	224.1	227	201.2	20	97.6	166.6	89.3	63.5	**111**
Θ-13	47.0	128.3	100.7	219.8	224	199.1	17	96.1	165.2	87.4	62.3	**121**
Θ-13N	42.0	131.5	104.2	231.5	233	206.7	27	111.0	178.3	95.0	72.2	**125**
N-15	50.0	133.8	106.7	228.7	231	202.9	17	94.3	163.6	87.8	60.2	**125**
N-15	50.2	133.8	106.7	267.2	261	224.2	13	117.7	184.1	93.3	66.6	**125-128**
N-16	45.0	108.9	79.5	262.4	258	218.0	21	117.8	184.2	93.2	67.3	**101**
N-14	41.5	131.4	104.1	243.4	243	208.9	19	114.7	181.5	89.9	66.7	**120**
ΠΘ-14	49.5	125.1	97.2	241.6	241	212.4	12	100.4	169.0	90.4	62.3	**110**
ΠΘ-14	49.6	134.6	107.6	258.0	254	220.5	12	121.5	187.4	91.9	68.2	**127**
ΠΘ-15	46.8	135.3	108.4	265.1	260	224.7	11	120.8	186.7	92.9	67.6	**127**

References:
(i) Fournier, 1977, (ii) Fournier, 1977, (iii) Arnórsson et al., 1983, (iv) Nieva and Nieva, 1987, (v) Fournier and Truesdell, 1983, (vi) Fournier and Potter, 1979, (vii) Fouillac and Michard, 1981, (viii) Kharaka et al., 1982, (ix) Giggenbach, 1988, (x) Kharaka and Mariner, 1989

The application of the CCG methodology has provided the following results:

- Chalcedony and quartz are close to equilibrium and they are candidate minerals for the reservoir wall rock.
- The estimated reservoir temperatures range from 83 to 120°C and the vast majority of them are higher than 110°C.
- The deep reservoir temperature is estimated to be around 120°C with a deviation of about 10-15°C and it is in good agreement with the values obtained by other chemical geothermometers, such as:
  (a) chalcedony geothermometer (Fournier, 1977): 100-105°C
  (b) quartz geothermometer - no steam loss (Fournier, 1977): 120-130°C
  (c) Na/Li geothermometer (Fouillac and Michard, 1981): 110-120°C

Water samples from production well TH-ΔB1 can be considered to be the most representative because (a) the water comes from the hot aquifer without mixing with shallow cold waters and (b) this well is located close to the upflow zone (Figure 2). The application of classic chemical geothermometers and the CCG method to the water samples from well TH-ΔB1 has provided the following results:

(i) quartz geothermometer - no steam loss (Fournier, 1977): 131.8-132.9°C
(ii) quartz geothermometer (Arnórsson et al., 1998): 119.4-120.6°C
(iii) chalcedony geothermometer (Fournier, 1977): 104.5-105.8°C
(iv) Na/Li geothermometer (Fouillac and Michard, 1981): 107.1-108.7°C
(v) K/Mg geothermometer (Giggenbach, 1988): 97.2-97.7°C
(vi) CCG method: 119-125°C

In the central part of the Strymon basin (Figure 1), north and northeast of the Therma-Nigrita geothermal field, deep hydrocarbon exploration boreholes have been drilled. The temperatures of 135 and 96°C were recorded at depths of 3,651 and 3,144m in borehole STR-1 and STR-3 respectively (Karytsas, 1990). These temperatures were measured at the basal breccias (bottom of the Miocene sediments) and the top of the basement. The deep reservoir temperature of 120°C (deviation of about 10-15°C) estimated by the CCG method is in accordance with the deep geothermal conditions in the central part of the Strymon basin suggesting 'the deep basin (reservoir) conceptual model' (Sorey et al., 1983) for the Therma-Nigrita hydrothermal-convection system.

3.2 Akropotamos Geothermal Field (Strymonikos Gulf, Eastern Macedonia)

The Akropotamos low enthalpy geothermal is located in the eastern coastal zone of the Strymonikos Gulf (Figure 1). The geological basement in the area is made up of gneisses, amphibolites, schists and marbles (Figure 3). Tertiary granitoids have intruded into the metamorophic rocks. The sedimentary sequence consists of basal conglomerates, sands, coarse-grained sandy marls, sandstones, thick-bedded biogenic limestones, marine sands, clays, travertines and calcarenites. Southwards, the entire series is covered with recent coastal and fluvial-torrential deposits and scree. The area is dominated by NW-SE and NE-SW faults and has been influenced by the presence of the North Anatolia Fault Zone (Kolios et al., 2010).

Six (6) large-diameter wells (AKR-1 to AKR-6), 275-545m deep, were constructed some years ago (Figure 3). The deeper reservoir is located 515m below surface, providing fluids of 90°C, whereas shallower reservoirs exist at depths of 130m (46°C) and 230m (85°C). Recently, long term production tests were performed in two of the existing geothermal wells, that showed high rate artesian flow (AKR-1: 220-230 m^3/h, AKR-3: 150-160 m^3/h) and produced CO$_2$-rich fluids with temperatures 84-90°C (Papachristou et al., 2019). The waters with temperatures of 30-90°C and TDS of 2.1-30.7 g/l belong to the Na-CI and Na-HCO$_3$ types and can be divided into two categories based on their salinity, i.e. higher and lower salinity waters (Arvanitis et al., 2016). The contribution of sea water to the chemical compositions of the thermal waters in the shallow aquifer system seems important (Arvanitis et al., 2016).

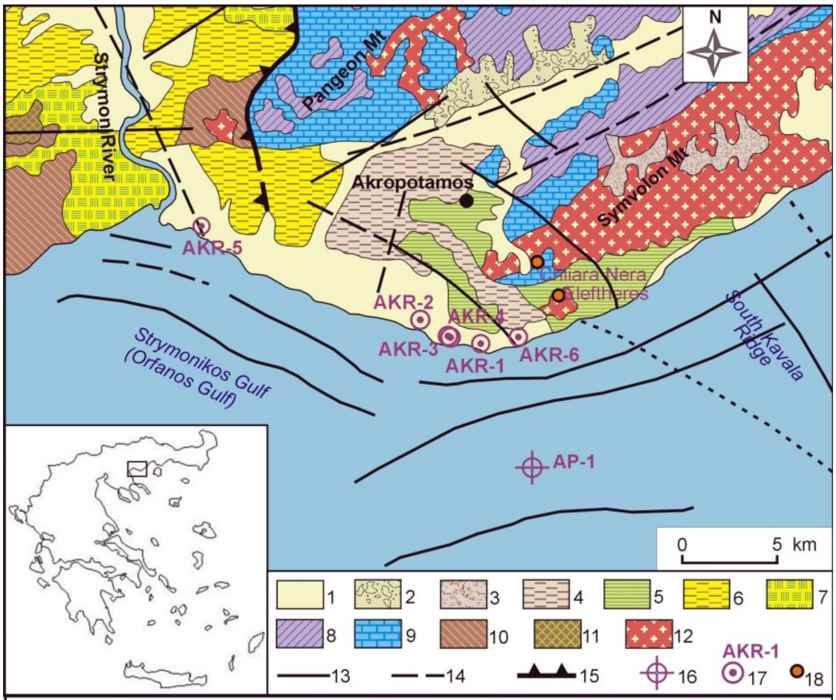

1: Alluvial deposits in valleys & coastal deposits, 2: Alluvial fans & older talus cones - Scree, 3: Pleistocene lacustrine & continental deposits (clays, loams, sands, conglomerates, 4: Pleistocene marine deposits (marls, clays, sands, conglomerates, coastal terraces), 5: Pliocene marine sediments (conglomerates, sands, clays, marls, marly limestones), 6: Mio-Pliocene lacustrine & terrestrial sediments (conglomerates, sands, marls, clayey material, marly limestones and clays), 7: Mio-Pliocene marine sediments (the above-mentioned detrital sediments), 8: Amphibolites, gneisses, schists with marble intercalations (Rhodope Massif), 9: Marbles or crystalline limestones (Rhodope Massif), 10: Amphibolites, gneisses, schists with some marble intercalations (Serbomacedonian Massif), 11: Gneisses (Serbomacedonian Massif), 12: Tertiary granitoids, 13: Fault, 14: Probable fault, 15: Strymon tectonic line, 16: Oil exploration borehole, 17: Geothermal well, 18: Thermal spring].

Figure 3: Simplified geological map of the Akropotamos area with the locations of geothermal wells, thermal springs and off-shore hydrocarbon exploration borehole AP-1 (Kolios et al., 2010; Arvanitis et al., 2016).

The results of the chemical analyses, as well as the temperature of the water samples from geothermal production wells and thermal springs (Kolios et al., 2006; Athanassoulis et. al., 2009) are presented in Table B (Appendix). The Computational Chemical Geothermometer was applied for all these samples. Nineteen (19) minerals are examined as candidates. The results of the CCG methodology, i.e. the candidate minerals and the estimated deep reservoir temperatures, are presented in Table 5. The application of the CCG methodology has given the following results:

- Candidate minerals for the reservoir wall rock are adularia, low albite, analcime, chalcedony, Mg-chlorite, laumontite, microcline and quartz.
- The estimated reservoir temperatures range from 58.5 to 112°C.

- The deep reservoir temperature is estimated to be around 110-120°C.

Table 5: Estimated deep reservoir temperatures and candidate minerals at the Akropotamos geothermal field (numbers 1, 2, 3, 6, 7, 10, 11, 18 and 21 represent adularia, low albite, analcime, chalcedony, Mg-chlorite, laumontite, microcline, prehnite and quartz respectively)

Water Samples	**Well AKR-1**	**Well AKR-2**	**Well AKR-4**	**Well AKR-4**	**Well AKR-5**	**Well AKR-6**	**Eleftheres Springs**	**Eleftheres Springs**	**Chliara Nera Springs**
Temp.	**112°C**	**72-75°C**	**90°C**	**90°C**	**58-78°C**	--	**94°C**	**85-87°C**	**92-111°C**
	Minerals	**Minerals**	**Minerals**	**Minerals**	**Minerals**	**Minerals**	**Minerals**	**Minerals**	**Minerals**
40°C					6, 21, 1, 10				
50°C		2, 3, 6, 11, 21	6, 21, 11	6, 21, 11		6, 21, 11	6, 21, 11	2, 6, 21, 11	3, 6
60°C					6, 21, 2, 3, 11				
70°C		6, 21	6, 21	6, 21		6, 21	6, 21	6, 21, 11	6
80°C					6, 21				
90°C	6, 21	6, 21	6, 21	6, 21		7, 21	6, 21	6, 21	6, 21
110°C	6, 21								
130°C	6, 21								
Comments	mixing: same results		mixing has no effect	mixing has no effect	no mixing	**failure**			

Table 6: Deep reservoir estimated temperatures at the Akropotamos geothermal field using both classical chemical geothermometers and the Comprehensive Computational Chemical Geothermometer (CCG)

Water Samples	**T(°C)**	**SiO_2 quartz** (i)	**SiO_2 chalcedony** (ii)	**Na/K** (iii)	**Na/K** (iv)	**Na-K-Ca** (v)	**Na-K-Ca, Mg correction** (vi)	**Na-Li** (vii)	**Na-Li** (viii)	**K-Mg** (ix)	**Li-Mg** (x)	**CCG**
Well AKR-1	83.0	121.5	93.2	176	188	195	140	--	--	135	--	**112**
Well AKR-2	46.0	82.5	51.3	77	102	127	10	--	--	63	--	**72-75**
Well AKR-4	48.0	93.5	63.0	108	130	169	2	--	--	95	--	**90**
Well AKR-4	48.0	93.5	63.0	125	144	179	2	--	--	98	--	**90**
Well AKR-5	30.0	65.8	33.8	64	90	133	3	--	--	74	--	**58-78**
Well AKR-6	38.0	27.7	-5.2	91	115	151	8	--	--	91	--	**---**
Eleftheres Springs	41.0	97.8	67.6	176	188	173	125	110.8	178.1	101	91	**94**
Eleftheres Springs	41.4	96.6	66.2	187	197	185	127	85.5	155.7	112	86	**85-87**
Chliara Nera Springs	52.0	131.4	104.1	237	238	235	20	85.3	155.6	112	72.5	**92-111**

References:
(i) Fournier, 1977, (ii) Fournier, 1977, (iii) Arnórsson et al., 1983, (iv) Nieva and Nieva, 1987, (v) Fournier and Truesdell, 1983, (vi) Fournier and Potter, 1979, (vii) Fouillac and Michard, 1981, (viii) Kharaka et al., 1982, (ix) Giggenbach, 1988, (x) Kharaka and Mariner, 1989

Table 6 presents the calculated deep reservoir temperatures based on the CCG methodology compared to values obtained using other literature geothermometers. The Na/K geothermometer proposed by Arnorrson et al. (1983) yields temperatures of 64-237°C. The Na-K geothermometer developed by Nieva and Nieva (1987) provided temperatures of 90-238°C. The Na-K-Ca yields values in the range of 133-235°C. Unreliable temperatures are given by the Mg-correction for the Na-K-Ca geothermometers due to the wide range of their values (2-140°C). The Na-Li geothermometer developed by Fouillac and Michard (1981) gives temperatures of 85.3-110°C which are significantly lower than those provided by the Na-Li geothermometer proposed by Kharaka et al. (1982). The quartz geothermometers (Fournier, 1977) compute values of 65-131°C. Waters from geothermal wells (AKR-1, AKR-2, AKR-3, AKR-4, AKR-5, AKR-6) and the thermal springs plotted on the Giggenbach (1988) trilinear diagram show the following results: (a) Samples AKR-2, AKR-3, Eleftheres and Chliara Nera are plotted in the area of ‘immature waters’. Immature waters show that there is no water-rock equilibrium and therefore the use of the Na/K geothermometer is unsuitable and the estimations of the deep reservoir temperatures using cation geothermometers should be interpreted with caution. For not too acid waters, the K-Mg geothermometer may be used and its application to the above-mentioned geothermal waters gives temperatures of 63-135°C. (b) Samples AKR-1, AKR-4, AKR-5 and AKR-6 are plotted in the ‘partial equilibrium’ field and their position on this diagram indicates probable deeper reservoir temperatures in the ranges of 80-130°C (at shallower levels, t_{km}) and 120-215°C (at considerable depth, t_{kn}). Taking into account the temperatures calculated by various chemical geothermometers, the predicted deep reservoir temperatures range from 100 to 150°C or probably even higher. The increased SiO_2 content of the sample AKR-1 indicates its deeper origin (the solubility of SiO_2 increases with increasing temperature up to 340°C) and probably reflects the reservoir conditions. Therefore, the calculated value of 121.5°C (Table 6) seems to be very probable and realistic. In addition, the temperature of 121-130°C was measured at a depth of 3,146 m in offshore deep oil exploration borehole AP-1 (Figure 3; Arvanitis et al., 2016). The deep reservoir temperature of 110-120°C proposed by the CCG methodology is in agreement with that of the quartz geothermometer and the geothermal conditions of the wider area.

3.3 Eratino-Chrysoupolis Geothermal Field (Nestos Delta Basin, Eastern Macedonia)

The Eratino-Chrysoupolis low enthalpy geothermal field is located at the western part of the Delta Nestos basin (Figure 1). The basement is mainly composed of gneisses, amphibolites and marbles. The geothermal anomaly coincides with the Eratino tectonic horst, southeast of the Eratino village (Figure 4). The geothermal reservoir is found at the depths of 485-670m, beneath a thick sequence of relatively impermeable sediments. It is made up of sandstones, oolithic and micritic limestones, micro-conglomerates and cemented gravels (calcarenite formation) with thin intercalations of clays and marls. The water temperature in this reservoir is 75°C. Geothermal production wells N1-P and N-2P (Figure 4) reached the depth of 655 and 670m and yield waters of 65 and 55°C, respectively (Kolios et al., 2005; Kolios et al.; 2007).

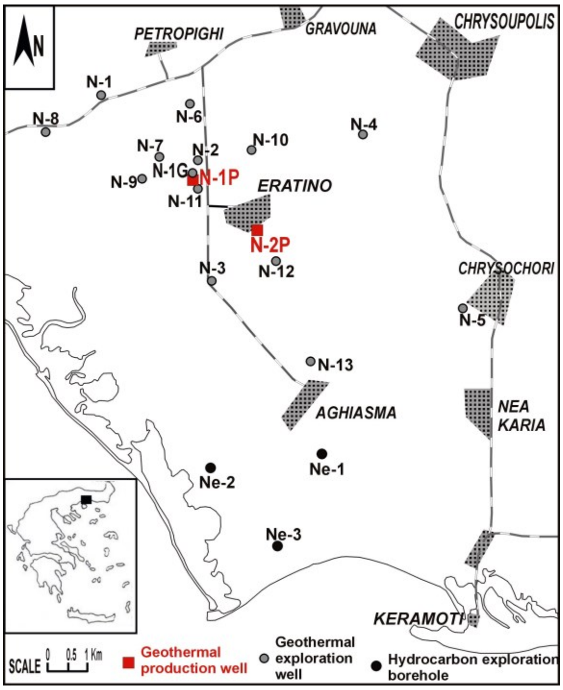

Figure 4: Map of the Eratino-Chrysoupolis geothermal filed with the locations of geothermal production wells and exploration boreholes (Kolios et al., 2005).

The geothermal waters belong to the Na-Cl group. Their salinity is relatively high (12.6-15.2 g/l), due to circulation in marine-brackish sediments and enrichment with ions (Kolios et al., 2005). These saline waters are highly corrosive to metals. The thermal waters may have circulated to great depths and are probably extracted from the transitional zone between the shallow geothermal reservoir at 550m depth and the overlying relatively impermeable sediments.

The Computational Chemical Geothermometer was applied for wells N-1P and N-2P. The results of the chemical analyses from these wells along with the water temperatures (Kolios et al., 1999; Kolios et al., 2005) are presented in Table C (Appendix). Various minerals are examined as candidates. The results of the CCG methodology, i.e. the candidate minerals and the estimated deep reservoir temperatures, are presented in Table 7. The application of the CCG methodology has given the following results:

- Candidate minerals for the reservoir wall rock are chalcedony and quartz.
- The estimated reservoir temperatures range from 71.8 to 83°C.
- The deep reservoir temperature is estimated to be around 80°C.
- The estimated temperature of 80°C is almost similar to the value of 75°C measured in the penetrated reservoir.

Table 7: Deep reservoir estimated temperatures and candidate minerals at the Eratino-Chrysoupolis geothermal field (numbers 6 and 21 represent Chalcedony and Quartz respectively)

Water Samples	Well N-1P	Well N-2P
Temp.	**83°C**	**71.8°C**
	Minerals	**Minerals**
70°C		6, 21
90°C	6, 21	6, 21
110°C	6, 21	6, 21
130°C	6, 21	

Table 8 presents the calculated deep reservoir temperatures based on the CCG methodology compared to values obtained using other classic geothermometers. The Na/K geothermometer, proposed by Arnorrson et al. (1983), gives underestimated and unreliable temperatures, since the computed value for well N-1P is lower than the measured one. The Na-K geothermometer, developed by Nieva and Nieva (1987) provided temperatures of 85-92°C (slightly higher than those which are measured in the reservoir). The Na-K-Ca yields even higher values (114-120°C). Underestimated temperatures (<75°C) are resulted from the Mg-correction for the Na-K-Ca geothermometers, as well as from the chalcedony (Fournier 1977), Li-Mg (Kharaka and Mariner, 1989) and Na-Li (Fouillac and Michard, 1981) geothermometers. The quartz (Fournier, 1977) and Na-Li (Kharaka et al., 1982) geothermometers provide values of 82-92°C. The K-Mg geothermometer (Giggenbach, 1988) gives temperatures of 79°C. Both water samples are plotted in the 'partial equilibrium' field on the Giggenbach (1988) trilinear diagram and their positions on this diagram indicate probable deeper reservoir temperature of 100°C. It should be noted that a larger number of geothermal water sample analyses are required for more accurate estimates.

Table 8: Deep reservoir estimated temperatures at the Eratino-Chrysoupolis geothermal field using both classical chemical geothermometers and the Comprehensive Computational Chemical Geothermometer (CCG)

Water Samples	T(˚C)	SiO_2 quartz (i)	SiO_2 chalcedony (ii)	Na/K (iii)	Na/K (iv)	Na-K-Ca (v)	Na-K-Ca, Mg correction (vi)	Na-Li (vii)	Na-Li (viii)	K-Mg (ix)	Li-Mg (x)	CCG
Well N-1P	65.0	90.3	60	58	85	114	71	11.5	85.6	79	60.3	**83**
Well N-2P	55.0	82.2	51	67	92	120	61	17.6	91.6	79	60.9	**71.8**

References:
(i) Fournier, 1977, (ii) Fournier, 1977, (iii) Arnórsson et al., 1983, (iv) Nieva and Nieva, 1987, (v) Fournier and Truesdell, 1983, (vi) Fournier and Potter, 1979, (vii) Fouillac and Michard, 1981, (viii) Kharaka et al., 1982, (ix) Giggenbach, 1988, (x) Kharaka and Mariner, 1989

Deep geothermal exploration borehole N-1G was drilled in the zone of the highest thermal gradient (Figure 4). The temperature of 122°C was measured at depth of 1,377m. This value suggests the existence of a deeper geothermal reservoir (in the basement) that probably contains medium enthalpy fluids. Moreover, three deep hydrocarbon exploration boreholes (Ne-1, Ne-2 and Ne-3 to corresponding depths of 3,159, 3,970 and 3,851m) were drilled south of the Eratino-Chrysoupolis geothermal field (Figure 4). The temperatures of 126.4, 164 and 160°C were recorded at depths of 3,156, 3,960 and 3,851m in boreholes Ne-1, Ne-2 and Ne-3 respectively (Kolios et al., 2007; Kolios et al., 2010).

3.4 Neo Erasmio - Magana Geothermal Field (Nestos Delta Basin, Thrace)

The Neo Erasmio - Magana geothermal field is located at the eastern part of the Nestos basin (Figure 1). This is a typical example where the stratified aquifers are fed by hot waters which rise through active faults that affect the basement. The metamorphic basement is made up mainly of migmatitic gneisses. In the area of the village of Neo Erasmio (Figure 5), the thermal fluids rise from a deeper reservoir within the metamorphic basement through a NNW-SSE trending fault system. During their ascent the fluids enter the sediments that act as confined aquifers. Subsequently, the hot fluids have a lateral flow towards the permeable formations causing an E-W extension of the geothermal anomaly. The geothermal reservoir is located at depths of 150-500m, at the basal part of the post-alpine sedimentary sequence (conglomerates, sandstones) and at the top of the basement. It contains waters of 30-68°C (Kolios et al., 2005).

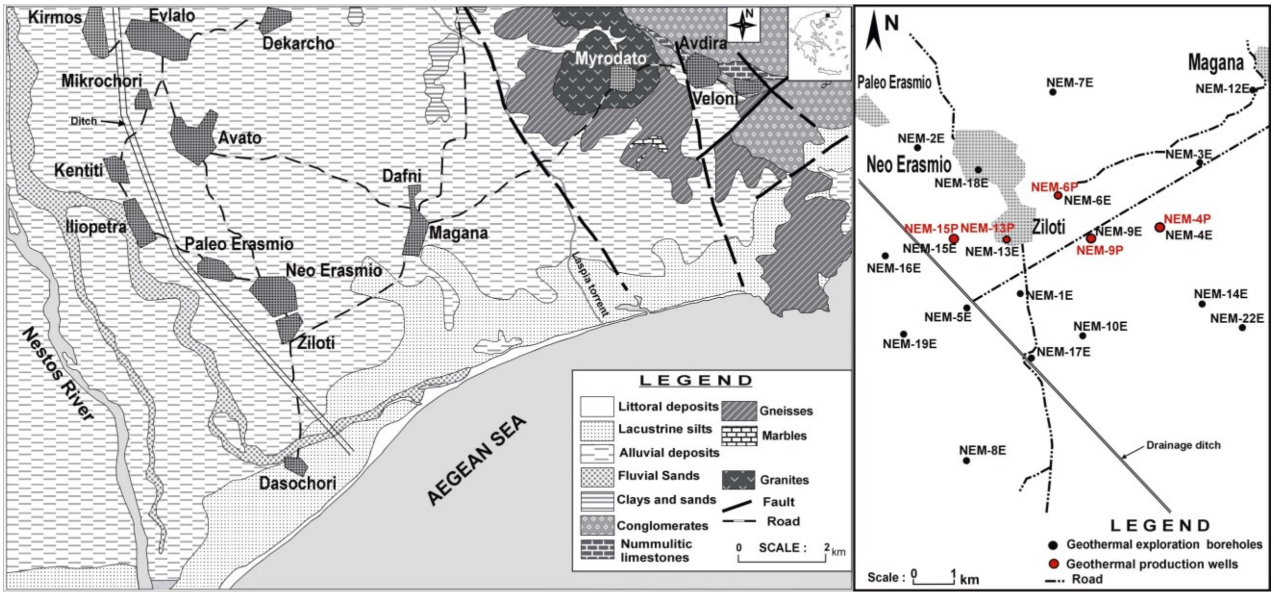

Figure 5: (Left) Geological map of the Neo Erasmio-Magana area. (Right) Map of the Neo Erasmio-Magana geothermal field with the locations of geothermal production and exploration wells (Kolios et. al., 2005).

The geothermal waters in the Neo Erasmio-Magana field, with TDS values between 0.57 and 10.1 g/l, are classified into two main categories: Na-Cl and Na-HCO_3Cl. The waters of the first group (NEM-4P, NEM-6P, NEM-9P, NEM-5E, NEM-10E, NEM-18E) are brackish with high Na^+ and Cl^- concentrations, due to the marine origin of the Paleogene sediments, which may preserve fossil saline waters and brines. During their lateral flow, the hot waters enter these Paleogene aquifers and they are probably enriched in Na^+ and Cl^- ions. Such waters are found in the eastern part of the field. The waters NEM-13P, NEM-15P, NEM-1E, NEM-3E and NEM-16 of the second group (Na-HCO_3Cl) are characterized by low salinities (0.57-1.17 g/l) and they occur mainly in the western part of the field (Kolios et al., 2005).

The Computational Chemical Geothermometer was applied for the water samples from geothermal production and exploration wells. The results of chemical analyses along with the temperatures (Kolios and Karydakis, 2000; Kolios et al., 2005) are summarized in Table D (Appendix). Various minerals are examined as candidates. The results of the CCG methodology are presented in Table 9. In some cases, the application of the CCG methodology has failed. The application of the CCG methodology has given the following results:

- Candidate minerals for the reservoir wall rock are mostly chalcedony and quartz.
- The estimated reservoir temperatures range from 49.5 to 96°C.
- The deep reservoir temperature is estimated to be 90-100°C.

Table 9: Deep reservoir estimated temperatures and candidate minerals at the Neo Erasmio-Magana geothermal field (numbers 2, 3, 6, 11 and 21 represent low albite, analcime, chalcedony, microcline and quartz respectively)

Water Samples	Well NEM-13P	Well NEM-15P	Well NEM-6P	Well NEM-6E	Well NEM-9P	Well NEM-9E	Well NEM-4P
Temp.	**50.7°C**	**49°C**	**71.6-92.5°C**	**95.4°C**	**95.2°C**	**96°C**	**71.7°C**
	Minerals	**Minerals**	**Minerals**	**Minerals**	**Minerals**	**Minerals**	**Minerals**
50°C							
60°C							6, 21
70°C							
80°C	6, 21	6, 21	6, 2, 3	6, 21	6, 21	6, 21	6, 21
90°C							
100°C	6, 21	6, 21	6, 21	6, 21	6, 21	6, 21	6, 21
110°C							
120°C	6, 21	6, 21	6, 21	6, 21	6, 21	6, 21	
130°C							
Comments	**failure** - zero mixing	**failure** - zero mixing	no mixing	zero mixing	zero mixing	zero mixing	zero mixing

Water Samples	Well NEM-1E	Well NEM-3E	Well NEM-5E	Well NEM-10E	Well NEM-18E	Well NEM-13E
Temp.	**49.5°C**	**47.0°C**	**62.4°C**	**61.5-66.3°C**	**> 150°C**	**96°C**
	Minerals	**Minerals**	**Minerals**	**Minerals**	**Minerals**	**Minerals**
50°C		6, 21				
60°C				6, 21, 11		
70°C	6, 21	6, 61			6, 21	
80°C			6, 21	6, 21		
90°C	6, 21	6, 21			6, 21	6, 21
100°C			6, 21	6, 21		
110°C	6, 21				6, 21	6, 21
120°C			6, 21			
130°C						6, 21
Comments	zero mixing	zero mixing	**failure** - probable mixing	zero mixing	**failure**	mixing coef.<0.05, mixing does not affect mineral's selection

Table 10 presents the calculated deep reservoir temperatures based on the CCG methodology compared to values obtained using other classic geothermometers. All water samples are plotted in the 'partial equilibrium' field on the Giggenbach (1988) trilinear diagram and their positions on this diagram indicate probable deeper reservoir temperatures in the range of 80-210°C, while the vast majority lies between the curves of 80 and 160°C. The Na/K and Na-K-Ca geothermometers gives temperatures of 20-185°C (usually >100°C). Mg-correction for the Na-K-Ca geothermometers yields similar temperatures (91-168°C). The Na-Li geothermometer proposed by Kharaka et al. (1982) suggest temperatures ranging from 117 to 152°C. Significantly lower values (44-81°C) are calculated by the Na-Li geothermometer presented by Fouillac and Michard (1981) for Cl<0.3 mol/kg. The Li-Mg geothermometer (Kharaka and Mariner, 1989) provides values varying between 70-134°C. The water sample from well NEM-6P provides negative values for all Li-based geothermometers. The temperatures from the K-Mg geothermometer (Giggenbach, 1988) are 52-161°C. The chalcedony geothermometer (Fournier, 1977) gives underestimated temperatures (18-93°C) and, in many cases, the calculated values are lower than the measured water temperatures. The values calculated using the quartz geothermometer (no steam loss - conductive cooling) range from 50-122°C. The comparison of the obtained values between the CCG methodology and the literature quartz geothermometer (Fournier, 1977) shows that there is a satisfactory agreement between them.

Table 10: Deep reservoir estimated temperatures at the Neo Erasmio geothermal field using both classical chemical geothermometers and the Comprehensive Computational Chemical Geothermometer (CCG) (f: failure)

Water Samples	T(°C)	SiO_2 quartz (i)	SiO_2 chalcedony (ii)	Na/K (iii)	Na/K (iv)	Na-K-Ca (v)	Na-K-Ca, Mg correction (vi)	Na-Li (vii)	Na-Li (viii)	K-Mg (ix)	Li-Mg (x)	CCG
NEM-13P	66.5	88	56	63	89	116	104	62	134	81	89	**50.7** (f)
NEM-15P	68.0	84	52	69	94	118	34	81	152	62	76	**49.0** (f)
NEM-6P	64.0	118	90	20	49	81	81	-91	-25	79	-5	**71.6-92.5**
NEM-6E	64.0	107	77	105	127	142	142	--	--	117	--	**95.4**
NEM-9P	60.0	109	79	165	179	185	185	--	--	161	--	**95.2**
NEM-9E	60.8	122	93	125	144	159	159	68	140	152	134	**96.0**
NEM-4P	42.0	75	43	98	121	138	127	53	125	102	90	**71.7**
NEM-1E	53.5	77	45	26	54	74	74	53	126	52	73	**49.5**
NEM-3E	30.4	57	25	92	115	117	50	--	--	71	--	**47.0**
NEM-5E	62.1	71	39	64	90	68	68	44	117	74	72	**62.4** (f)
NEM-10E	47.0	79	47	81	106	97	97	50	123	76	70	**61.5-66.3**
NEM-18E	52.5	50	18	60	86	106	102	--	--	75	--	**> 150** (f)
NEM-13E	66.6	92	61	66	91	110	98	--	--	76	--	**96**

References:
(i) Fournier, 1977, (ii) Fournier, 1977, (iii) Arnórsson et al., 1983, (iv) Nieva and Nieva, 1987, (v) Fournier and Truesdell, 1983, (vi) Fournier and Potter, 1979, (vii) Fouillac and Michard, 1981, (viii) Kharaka et al., 1982, (ix) Giggenbach, 1988, (x) Kharaka and Mariner, 1989

3.5 Aristino - Alexandroupolis Geothermal Field (Delta Evros Basin, Thrace)

The Aristino - Alexandroupolis geothermal field is located east of Alexandroupolis, at the western margins of Delta Evros Basin (Figure 1) near the well-known Traianoupolis thermal springs (Figure 6). The geothermal anomaly is associated with a combination of magmatism and active tectonics. The geothermal reservoir, composed of altered volcanic rocks and pyroclatics (ignimbrites), is found at the depths 200-400m (Kolios et al., 2005). The exploration and production wells that have been drilled in the area produce waters with temperatures up to 99^{o}C.

The geothermal waters belong to the Na-Cl type. Their TDS values range between 4.3 and 10.5 g/l and their Ca^{2+} and SO_4^{2-} contents are relatively high. The waters from the Traianoupolis thermal spring belong to the same type. The waters coming from the upper aquifer zone (around 200m deep) have a similar chemical composition with ones from the deeper aquifer (>350m). The hot waters in the area of wells EB-1, EB-2 and EB-3 (Figure 6) are of Na-SO_4 type and they come from a local shallow reservoir heated by conduction. These waters are of meteoric origin and their mineralization is due to hydrolysis of argillo-siliceous minerals. The higher temperature hydrothermal solutions of the Na-CI type is suggested as a result of the mixing of meteoric origin waters with deeper thermal solutions in which the marine component dominates (Poutoukis and Dotsika, 1998; Kolios et al., 2005).

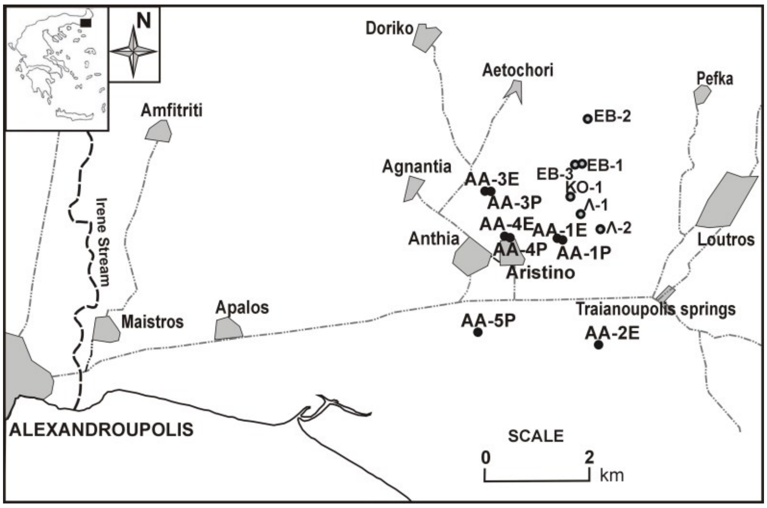

Figure 6: Map of the Aristino-Alexandroupolis geothermal filed with the locations of geothermal wells and thermal springs (Kolios et al., 2005)

The results of chemical analyses along with the temperatures of water samples from geothermal (production and exploration) wells and the Traianoupolis thermal spring (Kolios, 2001; Kolios et al., 2005; Poutoukis and Dotsika, 1988) are presented in Table E (Appendix). The Computational Chemical Geothermometer was tested against geothermal data included in this Table. Nineteen (19) minerals (summarized in Table 3) were examined. The criterion for considering a mineral as a candidate for the reservoir was the estimated R_{kj} value at the water temperature to be in the range 0.15-7. The results of the CCG methodology are presented in Table 11. In some cases, the application of the CCG methodology has failed due to possible mixing phenomena.

Table 11: Deep reservoir estimated temperatures and candidate minerals at the Aristino-Alexandroupolis geothermal field (numbers 1, 2, 3, 6, 11 and 21 represent adularia, low albite, analcime, chalcedony, microcline and quartz respectively)

Water Samples	Well AA-1E	Well AA-1P	Well AA-2E	Well AA-3E	Well AA-3P	Well AA-4E	Well AA-4P[1]
Temp.	**96°C**	**59.1-79.7°C**	**49°C**	**70°C**	**60°C**	**58.5-60°C**	**60°C**
	Minerals	**Minerals**	**Minerals**	**Minerals**	**Minerals**	**Minerals**	**Minerals**
40°C							
50°C			6, 21				
60°C						6, 21, 11	
70°C		6, 21	6, 21				
80°C						6, 21	
90°C	6, 21	6, 21	6, 21	6, 21	6, 21		6, 21
100°C						6, 21	
110°C	6, 21	6, 21		6, 21	6, 21		6, 21
130°C	6, 21			6, 21	6, 21		6, 21
Comments	mixing coef.<0.05, mixing does not affect mineral's selection	no mixing, mixing: same results		**failure -** probable mixing	**failure -** probable mixing	**failure**	**failure -** probable mixing

Water Samples	Well AA-5P	Well EB-1	Well EB-3	Well KO-1	Well AA-E	Traianoupolis Springs
Temp.	**58.4-69°C**	**67.7°C**	**115°C**	**121°C**	**95.2°C**	**86.6°C**
	Minerals	**Minerals**	**Minerals**	**Minerals**	**Minerals**	**Minerals**
40°C						
50°C	6, 21, 1, 3					
60°C		6, 21				
70°C	6, 21, 11					6, 2, 21
80°C		6, 21				
90°C	6, 21			6, 21	6, 21	6, 21
100°C		6, 21				
110°C			6, 21	6, 21	6, 21	
130°C			6,21	6, 21	6, 21	6, 21
150°C			6,21			
Comments						

Table 12 presents the calculated deep reservoir temperatures based on the CCG methodology compared to values obtained using other literature geothermometers. All water samples (geothermal wells and Traianoupolis springs) are plotted in the 'partial equilibrium' field on the Giggenbach (1988) trilinear diagram and their positions on this diagram indicate probable deeper reservoir temperatures in the range of 100-190°C. The Na/K and Na-K-Ca geothermometers yield values 28-169°C but the vast majority ranges between 114-169°C. Mg-correction for the Na-K-Ca geothermometers gives similar temperatures (91-168°C). The Na-Li geothermometer proposed by Kharaka et al. (1982) provides temperatures of 124-197°C, which are considered to be overestimated. Lower values (51-133°C) are calculated by the Na-Li geothermometer presented by Fouillac and Michard (1981) for Cl<0.3 mol/kg. The Na/Li geothermometer is sensitive to TDS and rock type and slight changes in Li concentrations during the ascent of fluid can affect the Na/Li ratio since Li is a minor constituent and Na is a major one (D' Amore and Arnórsson, 2000). The Li-Mg geothermometer (Kharaka and Mariner, 1989) gives values higher than 100°C (101-146°C). The K-Mg geothermometer (Giggenbach, 1988) yields realistic temperatures (83-152°C). The chalcedony geothermometer (Fournier, 1977) is suitable for low temperature sources and gives temperatures of 38-101°C which can be considered underestimated (in some cases, the computed values are lower than the water temperature). The quartz geothermometer (no steam loss, conductive cooling) proposed by Fournier (1977) yields values ranging from 73.9 to 128°C. The geothermal waters are plotted on the Giggenbach and Coguel (1989) diagram (Powell and Cumming, 2010) and this plot shows that the probable deep temperatures vary between 80 and 130°C. According to Poutoukis and Dotsika (1988), the Na/K, K/Mg, Li/Mg and Na/Li geothermometers agree with the isotopic data attributing a temperature of 130-140°C for the deeper geothermal waters in the Aristino field.

The application of the CCG methodology has provided the following results:

- Candidate minerals for the reservoir wall rock are mainly chalcedony and quartz and in a few cases other candidate minerals, such as adularia, low albite, analcime and microcline, are added.
- The estimated reservoir temperatures range from 49 to 121°C.
- The deep reservoir temperature is estimated to be 100-120°C. These values are in good agreement with the ones obtained by some chemical geothermometers, especially the quartz geothermometer (Fournier, 1977). They are also relatively lower compared to those temperatures suggested by other literature geothermometers.

Table 12: Estimated deep reservoir temperatures at the Aristino-Alexandroupolis geothermal field using both classical chemical geothermometers and the Comprehensive Computational Chemical Geothermometer (CCG) (f: failure)

Water Samples	**T(°C)**	**SiO_2 quartz** (i)	**SiO_2 chalcedony** (ii)	**Na/K** (iii)	**Na/K** (iv)	**Na-K-Ca** (v)	**Na-K-Ca, Mg correction** (vi)	**Na-Li** (vii)	**Na-Li** (viii)	**K-Mg** (ix)	**Li-Mg** (x)	**CCG**
AA-1E	80.0	114	85	134	152	160	132	--	--	116	--	**96**
AA-1P	51.8	101	71	110	132	149	129	--	--	111	--	**59.1-79.7**
AA-2E	30.5	53	20	114	135	151	140	--	--	117	--	**49**
AA-3E	87.0	93	62	59	86	119	113	--	--	97	--	**70** (f)
AA-3P	89.0	70	38	99	122	144	144	--	--	128	--	**60** (f)
AA-4E	60.1	73	41	28	56	91	91	--	--	88	--	**60**
AA-4P[1]	64.0	78	46	34	62	96	96	72	143	90	121	**58.5-60** (f)
AA-5P	32.5	76	44	117	138	155	153	--	--	129	--	**58.4-69**
EB-1	42.5	85	54	68	94	114	105	--	--	83	--	**67.7**
EB-3	92.5	128	101	131	149	164	154	133	197	130	146	**115**
KO-1	82.5	128	101	133	151	168	168	--	--	152	--	**121**
AA-E	76.5	128	100	141	158	169	164	90	160	137	127	**95.2**
Traianoupolis Springs	51.0	94	63	145	162	171	163	51	124	135	101	**86.6**

References:
(i) Fournier, 1977, (ii) Fournier, 1977, (iii) Arnórsson et al., 1983, (iv) Nieva and Nieva, 1987, (v) Fournier and Truesdell, 1983, (vi) Fournier and Potter, 1979, (vii) Fouillac and Michard, 1981, (viii) Kharaka et al., 1982, (ix) Giggenbach, 1988, (x) Kharaka and Mariner, 1989

Hydrocarbon exploration boreholes DEV-1, DEV-2 and DEV-3 were drilled southeast of the Aristino geothermal field and the Traianoupolis springs. Borehole DEV-1 has a depth of 4,229m and the temperatures of 96, 136 and 146°C were measured at depths of 2,740, 3,975 and 4,229m respectively. The temperatures of 90 and 100°C were recorded at depths of 2,500 and 3,000m respectively in borehole DEV-2 (3,213m deep). Borehole DEV-3 reached the depth of 2,860m and the temperatures of 104 and 108°C were recorded at 2,650 and 2,860m respectively (Kolios et al., 2007; Kolios et al., 2010). These borehole temperatures are close to the deep reservoir temperatures that were estimated using both classical chemical geothermometers and the CCG methodology.

4. CONCLUSIONS

In this work a detailed and Comprehensive Computational Chemical Geothermometry (CCG) method is proposed based on the consideration of the equilibrium between geothermal water and specific minerals at a given temperature within deeper reservoir. This two-stage approach was applied to geothermal waters from significant low enthalpy geothermal fields in Northern Greece, i.e. Therma-Nigrita, Akropotamos, Eratino-Chrysoupolis, Neo Erasmio-Magana, Aristino-Alexandroupolis. The obtained results were compared to those from other classic geothermometers and the validity and reliability of the proposed CCG methodology was evaluated. The predictions of this model are in satisfactory agreement with the results of the geothermal exploration carried out in these areas. It is believed that this approach could be applied to reliably estimate deep reservoir temperatures in other areas as well.

The application of the Comprehensive Computational Chemical Geothermometer (CCG) to geothermal waters of the above-mentioned low enthalpy geothermal fields is important because these fields are of high interest for further development and future investments. The knowledge of the probable deep temperatures can contribute to the rational and optimal utilization of the geothermal resources in these areas. More specifically (Papachristou et al., 2019): (i) In the Therma-Nigrita low enthalpy geothermal field, the fluids are being used for greenhouse heating and Spirulina cultivation. Moreover, a distribution network for agricultural uses has been designed but it has not been completed yet. (ii) In the Akropotamos field, the Municipality of Paggaio (local authorities) has been awarded the rights to exploit the low temperature geothermal resources and plans to invest €10 million for district heating/cooling networks and the distribution of thermal energy to semi-urban settlements, greenhouses and spa resorts (this project is still in the early implementation phase). (iii) In the Eratino-Chrysoupolis field, the management rights have been leased to the Municipality of Nestos, which invested more than €10 million for the construction of the heat distribution infrastructure providing thermal energy to end users exclusively for agricultural use. The first 3.5 ha greenhouse unit has already been connected to the distribution network. (iv) In the Neo Erasmio-Magana field, the exploitation/management rights have been leased to a private company which gradually constructed 18.5 ha geothermal greenhouses with future expansion reaching 20 ha. The low temperature fluids are also used by another private company for the operation of a dehydration plant and soil heating for off-season asparagus cultivation. (v) In the Aristino-Alexandroupolis low temperature field, the Municipality of Alexandroupolis has leased the exploitation/management rights and is implementing a project which includes the construction of new deep production and reinjection wells, the operation of the first geothermal district heating in Greece and the distribution of heat for agricultural purposes (greenhouse heating). Moreover, these low enthalpy geothermal fields are located in sedimentary basins of Northern Greece, which are considered to be favorable areas for probable existence of medium enthalpy geothermal resources suitable for binary cycle power generation (Kolios et al., 2007). In March 2011, international open tenders took place for the leasing of the rights to explore the geothermal potential of four promising areas including Evros River Delta and Nestos River Delta basins. A consortium of two Greek private companies awarded all the tenders. In January 2012 another international open tenders took place concerning the exploration in other four areas including the Akropotamos field. Unfortunately, the lease contracts were never signed with the winners of the above-mentioned tenders and the tenders have been officially declared void (Andritsos et al., 2013; Andritsos et al., 2015). Based on more data, including estimated deep reservoir temperatures by applying chemical geothermometry techniques, the international open tenders may be repeated in the future. The contribution of CCG methodology to this direction is significant.

REFERENCES

Andritsos, N., Arvanitis, N., Dalabakis, P., Karytsas C., Mendrinos, D., and Papachristou, M.: Geothermal Energy Use, Country Update for Greece, *Proceedings*, European Geothermal Congress, Pisa Italy (2013)

Andritsos, N., Dalambakis, P., Arvanitis, A., Papachristou, M., and Fytikas, M.: Geothermal Developments in Greece - Country Update 2010-2014, *Proceedings*, World Geothermal Congress, Melbourne, Australia (2015)

Arnórsson, S., Sigurdsson, S., and Svavarsson H.: The Chemistry of Geothermal Waters in Iceland I. Calculation of Aqueous Speciation from 0°C to 370°C, *Geochim. Cosmochim. Acta*, **46**, (1982), 1513-1532.

Arnórsson, S., Gunnlaugsson E., and Svavarsson, H.: The Chemistry of Geothermal Waters in Iceland. III. Chemical Geothermometry in Geothermal Investigations, *Geochim. Cosmochim. Acta*, **47**, (1983), 567-577

Arnórsson, S., Andrésdóttir, A., Gunnarsson, I., and Stefánsson, A., New Calibration for the Ouartz and Na/K Geothermometers - Valid in the Range 0-350°C, *Proceedings*, Geoscience Society of Iceland Annual Meeting (April 1994), in Icelandic (1998), 42-43

Arvanitis, A., Fytikas, M., and Dotsika, E.: Geothermal Conditions in Therma - Nigrita Area (Strymon Basin, Northern Greece), *Bulletin of the Geological Society of Greece*, **32(4)**, (1998) 229-242

Arvanitis, A., Dotsika, E., and Kolios, N.: Geochemical Characteristics of the Geothermal Fluids in the Akropotamos Area (Macedonia, Northern Greece), *Bulletin of the Geological Society of Greece,* **50(2)**, (2016), 596-605

Athanassoulis, C., Vakalopoulos, P., Xenakis., M., Persianis, D., and Taktikos, S.: Periodic Monitoring of Curative Springs of Greece, Appendix, Technical/Scientific Report, I.G.ME., in Greek, Athens (2009).

D' Amore, F., and Arnórsson, S.: Geothermometry, In: Isotopic and Chemical Techniques in Geothermal Exploration, Development and Use: Sampling, Data Handling, Interpretation, Arnórsson, S. (Ed.), IAEA, Vienna, (2000), 152-199

Dimopoulos, G. C., Preliminary Hydrothermal - Geothermal Investigations of Nigrita Serres Geothermal Field (C. Macedonia, Greece), *Steir. Beitr.z.Hydrogeologie*, **41**, (1990), 133-148.

Fouillac, R., and Michard, S.: Sodium/Lithium Ratio in Water Applied to Geothermometry of Geothermal Reservoirs, *Geothermics*, **10**, (1981), 55-70

Fournier, R.O, and Truesdell, A.H.: An Empirical Na-K-Ca Geothermometer for Natural Waters, *Geochim. Cosmochim. Acta*, **37**, (1973), 1255-1275.

Fournier, R., White, O.D.E., and Truesdell, A.H.: Geochemical Indicators of Subsurface Temperature, 1, Basic Assumptions, *U.S. Geol. Survey Jour. Research,* **2**, (1974), 259-262

Fournier, R.O.: Chemical Geothermometers and Mixing Models for Geothermal Systems**,** *Geothermics*, **5**, (1977), 41-50.

Fournier, R. O.: A Revised Equation for the Na-K Geothermometer, *Geothermal Res. Council Trans.*, **3**, (1979), 221-224

Fournier, R. O., and Potter, R.W.II: Magnesium Correction to the Na-K-Ca Chemical Geothermometer, *Geochim. Cosmochim. Acta,* **37**, (1979), 1543-1550.

Giampaolo, C.C., Gorgoni, A. Mottana, Pagani, F., and Sighinolfi, G.: Experimental Water-Rock Interaction: Silica Geothermometers in the Temperature Range 100-350°C, *Europ. Jour. Mineral.*, **4**, (1992), 53-65.

Giggenbach, W.F., Gonfiantini, R., Jangi, B.L., and Truesdell, A. H.: Isotopic and Chemical Composition of Parbati Valley Geothermal Discharges, North-West Himalaya, India, *Geothermics*, **12**, 199-222 (1983).

Giggenbach, W.F.: Geothermal Solute Equilibria - Derivation of Na-K-Mg-Ca Geoindicators, *Geochim. Cosmochim. Acta*, **52**, (1988), 2749-2765.

Giggenbach, W.F., and Goguel, R.L.: Collection and Analysis of Geothermal and Volcanic Water and Gas Discharges, Report of Dep. of Sci. and Ind. Res., Chem. Div., Pentone, New Zealand (1989).

Hem, J.D. and Roberson, C.E.: Form and Stability of Aluminum Hydroxide Complexes in Dilute Solution, Geological Survey Water-Supply Paper 1827-A, U.S. Department of the Interior, Washington DC (1967).

Karydakis, G., Andritsos, N., and Fytikas, M.: Geothermal Energy Developments in the Prefecture of Serres, *Proceedings*, 6th National Conference on Renewable Energy Source (Volos, Greece, November 3-5, 1999), in Greek, Institute of Solar Technology, Thessaloniki (2000), A, 427-434.

Karydakis, G., Arvanitis, A., Andritsos, N., and Fytikas, M.: Low Enthalpy Geothermal Fields in the Strymon Basin (Northern Greece), *Proceedings*, World Geothermal Congress, Antalya, Turkey (2005)

Karytsas, C., Inventory of Low Enthalpy Geothermal Resources Discovered Through Deep Oil and Gas Exploration Wells, Centre for Renewable Energy Sources, Internal report for contract DG XVII 7030/ETD/89-6, Pikermi, Greece, (1990).

Kharaka, Y.K., Lico, M.S., and Law, L.M.: Chemical Geothermometers Applied to Formation Waters, Gulf of Mexico and California Basins, *Am. Assoc. Petrol. Geol. Bull.*, **66 (5)**, (1982), 588.

Kharaka, Y.K., and Mariner R.H.: Chemical Geothermometers and Their Application to Formation Waters from Sedimentary Basins, In: Thermal history of sedimentary basins, Naeser N.D. and McCulloh T.H. (Eds), Springer, New York, NY, (1989), 99-117.

Kolios, N., Koutsinos, S., Karydakis, G., and Zikopoulos, K.: Geothermal Reservoir Evaluation in the Nestos Delta Basin Based on the Results of Two Exploration-Production Wells in the Eratino-Chrysoupolis Area (Prefecture of Kavala), Technical Report, I.G.M.E., in Greek, Thessaloniki (1999).

Kolios, N., and Karydakis, G.: Geothermal Exploration in Neo Erasmio-Magana, Technical/Scientific Report, I.G.M.E., in Greek, Thessaloniki (2000).

Kolios, N.: Geothermal Exploration in the Aristino-Anthia Area (Prefecture of Evros), Technical/Scientific Report, I.G.M.E., in Greek, Thessaloniki (2001).

Kolios, N., Koutsinos, S., Arvanitis, A. and Karydakis, G.: Geothermal Situation in Northeastern Greece, *Proceedings*, World Geothermal Congress, Antalya, Turkey (2005)

Kolios, N., Koutsinos, S., Karydakis, G., and Arvanitis, A.: Results of Geothermal Exploration in the Akropotamos Area (Prefecture of Kavala), Technical/Scientific Report, I.G.M.E., in Greek, Thessaloniki, (2006).

Kolios, N., Fytikas, M., Arvanitis, A., Andritsos, N., and Koutsinos, S.: Prospective Medium Enthalpy Geothermal Resources in Sedimentary Basins of Northern Greece, *Proceedings*, European Geothermal Congress, Unterhaching-Germany (2007).

Kolios, N., Arvanitis, A., and Koutsinos S.: Investigation of possibility for power generation from medium temperature geothermal fluids in Macedonia and Thrace (Northern Greece), *Proceedings*, International Forum "Geothermal Energy in the Spotlight" - GES2009, in Greek, Thessaloniki, Greece, 11-12 December 2009, ISBN 978-960-6746-07-9, 38p. (2010).

Kolios, N., Arvanitis, A., Karydakis, G. and Koutsinos, S.: Geothermal Drilling Activity in the Akropotamos Area, *Bulletin of the Geological Society of Greece*, **43(5),** (2010), 2246-2256.

Nieva, D., and Nieva, R.: Developments in Geothermal Energy in Mexico, Part 12. A Cationic Geothermometer for Prospecting of Geothermal Resources, *Heat Recovery Systems and CHP*, **7**, (1987), 243-258.

Pang, Z.H., and Reed, M.: Theoretical Chemical Thermometry on Geothermal Waters: Problems and Methods, *Geochim. Cosmochim. Acta,* **62**, (1998), 1083-1091

Papachristou, M., Arvanitis, A., Mendrinos, D., Dalabakis, P., Karytsas, C. and Andritsos N.: Geothermal Energy Use, Country Update for Greece (2016-2019), *Proceedings*, European Geothermal Congress, Den Haag, (2019)

Parkhurst, D.L.: Ion-Association Models and Mean Activity Coefficients of Various Salts, In: Chemical Modeling of Aqueous Systems II (edited by D. C. Melchior and R.L. Bassett), ACS Symposium Series 416, ACS Washington, DC, 30-43(1990).

Pollak, W.H.: Structural and lithological development of the Prinos - Kavala basin, Sea of Thrace, Greece, *Annales Géologique des Pays Helléniques*, **2**, (1979) 1003-1011.

Poutoukis, D. and Dotsika, E.: Contribution of Isotope Hydrology and Hydrogeochemistry in the Study of the Geothermal Field of Aristino, Evros, *Bulletin of the Geological Society of Greece,* **32(4)**, in Greek (1998), 596-605

Powell, T., and Cumming, W.: Spreadsheets for Geothermal Water and Gas Chemistry, *Proceedings*, 35th Workshop on Geothermal Reservoir Engineering, Stanford University, Stanford, CA, USA, SGP-TR-188 (2010).

Reed, M.H.: Calculation of Multicomponent Chemical Equilibria and Reaction Processed in Systems Involving Minerals, Gases and An Aqueous Phase, *Geochim. Cosmochim. Acta,* **46**, (1982), 513-528.

Sorey, M.L., Nathenson, M., and Smith, C.: Methods for assessing low-temperature geothermal resources, In: Assessment of low-temperature geothermal resources of the United States - 1982, Geological Survey Circular 892, Prepared in cooperation with the U.S. Department of Energy, (1983), 17-30.

Spycher, N., Peiffer, L., Sonnenthal, E.L., Saldi, G., Reed, M.H., and Kennedy, B.M.: Integrated multicomponent solute geothermometry, *Geothermics*, **52**, 113-123 (2014).

Tole, M. P., Armannsson, H., Pang Zhong-He, and Arnórsson, S.: Fluid/Mineral Equilibrium Calculations for Geothermal Fluids and Chemical Geothermometry, *Geothermics*, **22**, 17-37 (1993).

Verros, G. D., Latsos, T., Anagnostou, K. E., Avlakiotis, P. Chaikalis, C., Liolios, C., Antoniou, D., Kotsopoulos, S., and Arsenos, P.: Physicochemical Characteristics of Thermopylae Natural Hot Water Springs in Central Greece: Chemical Geothermometry, *Proceedings,* American Institute of Physics Conf.., 963(2A) (2007), 412-415.

Verros, G.D., and Papachristou, M.: A Comprehensive Framework for Estimating the Reservoir Temperature by Chemical Geothermometry, *Proceedings*, 10th International Hydrogeological Congress of Greece, K. Voudouris et al., Geol. Soc. Greece, Thessaloniki, (2014), 749-757.

Verros, G.D., and Papachristou, M. Towards to the Development of a Detailed Computational Chemical Geothermometer, *Proceedings*, International Conference of Computational Methods in Sciences and Engineering (ICCMSE) 2017, Thessaloniki, AIP Conf. Proc. 1906, 200002-1–200002-5 (2017).

APPENDIX

Table A: Chemical analyses of the Therma-Nigrita geothermal waters (concentrations in mg/l) along with their temperatures (Dimopoulos, 1990; Arvanitis et al., 1998; Karydakis et al., 1999; Athanassoulis et al., 2009)

Ions	**Well TH-R1** T=59.8°C	**Well TH-R1** T=60.9°C	**Well TH-ΔB1** T=61.8°C	**Well TH-ΔB1** T=61.7°C	**Well TH-ΔB1** T=61.7°C	**Well TH-1** T=59.0°C	**Well TH-3** T=45.0°C	**Well TH-5** T=42.0°C	**Well TH-10** T=58.0°C	**Well TH-7** T=48.0°C
H^+	pH: 6.50	pH: 6.43	pH: 6.58	pH: 6.62	pH: 6.67	pH: 6.80	pH: 7.07	pH: 7.07	pH: 6.80	pH: 6.60
Na^+	567.0	581.0	654.0	665.0	655.0	528.7	533.3	524.1	537.4	46.1
K^+	136.0	139.0	95.1	93.4	92.6	82.1	97.8	90.0	92.2	13.4
Ca^{2+}	128.0	124.0	122.0	121.0	115.0	121.8	235.7	129.9	140.0	183.1
Mg^{2+}	90.4	87.3	80.5	79.0	75.2	95.3	105.0	109.4	90.9	92.4
SiO_2	78.0	75.6	90.6	91.7	92.6	71.0	50.4	55.8	**81.3**	35.8
CO_3^{2-}	0.0	0.0	0.0	0.0	0.0	0.0	0.0	0.0	0.0	0.0
HCO_3^-	2147.0	2158.0	2245.0	2265.0	2258.0	1963.4	2362.4	2025.8	2055.7	1104.0
SO_4^{2-}	140.0	150.0	165.0	175.0	165.0	104.7	141.7	139.3	115.9	9.6
Cl^-	165.0	165.0	191.0	170.9	184.0	157.75	150.66	152.4	156.9	30.2

Ions	**Well TH-11** T=51.0°C	**Well TH-11** T=42.4°C	**Well TH-11** T=46.2°C	**Well TH-11** T=46.0°C	**Well TH-11** T=46.1°C	**Well TH-11** T=47.6°C	**Well TH-11** T=47.4°C	**Well TH-11** T=48.0°C	**Well TH-11** T=49.2°C	**Well Θ-14** T=62.0°C
H^+	pH: 6.50	pH: 6.60	pH: 6.34	pH: 6.10	pH: 6.28	pH: 6.29	pH: 6.18	pH: 6.33	pH 6.55	pH: 7.24
Na^+	205.1	346.0	319.0	336.0	280.0	338.0	228.0	357.72	349.44	597.7
K^+	39.4	51.9	73.0	67.7	46.9	49.5	43.9	69.6	58.7	78.2
Ca^{2+}	116.4	90.8	92.7	89.9	110.0	85.0	154.0	109.0	99.4	140.3
Mg^{2+}	78.4	70.7	82.7	75.0	76.1	46.0	19.1	45.7	33.0	102.1
SiO_2	44.4	74.3	82.4	79.6	76.8	---	70.2	82.6	87.1	84.0
CO_3^{2-}	0.0	0.0	0.0	0.0	0.0	0.0	0.0	0.0	0.0	0.0
HCO_3^-	1214.0	1438.0	1428.0	1500.0	1285.0	1220.0	1028.0	1409.5	1159.3	2166.0
SO_4^{2-}	19.4	118.0	88.3	31.4	110.0	116.0	118.0	74.0	157.5	128.2
Cl^-	67.5	78.0	92.2	99.2	85.1	83.3	52.1	74.5	78.0	177.2

Ions	**Well Θ-13** T=47.0°C	**Well Θ-13N** T=42.0°C	**Well N-15** T=50.0°C	**Well N-15** T=50.2°C	**Well N-16** T=45.0°C	**Well N-14** T=41.5°C	**Spring ΠΘ-14** T=49.5°C	**Spring ΠΘ-14** T=49.6°C	**Spring ΠΘ-15** T=46.8°C
H^+	pH: 6.60	pH: 6.40	pH: 6.70	pH: 6.70	pH: 6.80	pH: 6.90	pH: 7.20	pH: 6.53	pH 6.56
Na^+	620.7	653.0	574.7	541.65	531.0	523.0	567.2	543.75	550.0
K^+	78.2	91.02	78.2	100.0	94.6	80.4	85.94	93.75	100.0
Ca^{2+}	148.3	141.0	138.3	99.0	137.1	131.1	100.2	93.25	88.75
Mg^{2+}	116.7	88.3	113.0	121.13	109.4	102.0	111.92	118.75	125.0
SiO_2	85.0	90.2	94.0	94.05	58.0	90.0	80.0	95.36	96.64
CO_3^{2-}	0.0	0.0	0.0	0.0	0.0	0.0	0.0	0.0	0.0
HCO_3^-	2252.6	2230.0	2112.9	2105.0	2074.0	2209.3	2021.9	2116.7	2141.1
SO_4^{2-}	129.7	159.0	125.8	120.0	130.0	128.0	130.77	72.52	96.06
Cl^-	177.2	163.0	170.2	170.76	153.6	155.8	156.03	170.4	152.65

Table B: Chemical analyses of the Akropotamos geothermal waters (concentrations in mg/l) along with their temperatures (Kolios et al., 2006; Athanassoulis et al., 2009)

Ions	**Well AKR-1** T=83.0°C	**Well AKR-2** T=46°C	**Well AKR-4** T=48.0°C	**Well AKR-4** T=48.0°C	**Well AKR-5** T=30.0°C	**Well AKR-6** T=38.0°C	**Eleftheres Thermal Springs** T=41.0°C	**Eleftheres Thermal Springs** T=41.4°C	**Chliara Nera Spring** T=52.0°C
H^+	pH: 6.85	pH: 7.28	pH: 6.13	pH: 6.64	pH: 7.55	pH: 7.35	pH: 6.20	pH: 7.30	pH: 7.20
Na^+	1700.0	750.0	8500.0	7668.0	9000.0	9600.0	650.0	678.2	1460.4
K^+	140	16.0	300.0	340.0	150.0	260.0	53.5	62.56	152.5
Ca^{2+}	127.45	28.86	343.89	367.0	436.07	881.76	212.5	120.24	34.47
Mg^{2+}	14.09	36.55	950.13	962.0	1231.5	946.24	19.25	12.64	93.33
SiO_2	74.6	32.3	41.7	41.7	21.3	6.9	45.84	44.6	90.0
CO_3^{2-}	0.0	0.0	0.0	0.0	0.0	0.0	0.0	0.0	0.0
HCO_3^-	1146.8	811.3	488.0	505.0	1549.0	30.5	1146.8	740.75	899.4
SO_4^{2-}	245.0	200.0	2445.0	2440.0	0.5	2590.0	25.0	143.13	240.64
Cl^-	2198.52	680.83	14538.6	14792.0	17659.0	16417.98	785.0	857.96	1318.85

Table C: Chemical analyses of the Eratino-Chrysoupolis geothermal waters (concentrations in mg/l) along with their temperatures (Kolios et al., 1999; Kolios et al., 2005)

Ions	**Well N-1P** T=65.0°C	**Well N-2P** T=55°C
H^+	pH: 7.08	pH: 7.45
Na^+	4500.0	3800.0
K^+	68.0	67.0
Ca^{2+}	861.72	681.36
Mg^{2+}	179.82	170.1
SiO_2	38.8	32.1
CO_3^{2-}	0.0	0.0
HCO_3^-	103.7	140.3
SO_4^{2-}	962.5	890.0
Cl^-	8510.4	6879.2

Table D: Chemical analyses of the Neo Erasmio-Magana geothermal waters (concentrations in mg/l) along with their temperatures (Kolios and Karydakis, 2000; Kolios et al., 2005)

Ions	**Well NEM-13P** T=66.5°C	**Well NEM-15P** T=68.0°C	**Well NEM-6P** T=64.0°C	**Well NEM-6E** T=64.0°C	**Well NEM-9P** T=60.0°C	**Well NEM-9E** T=60.8°C	**Well NEM-4P** T=42.0°C	**Well NEM-1E** T=53.5°C	**Well NEM-3E** T=30.4°C	**Well NEM-5E** T=62.1°C	**Well NEM-10E** T=47.0°C	**Well NEM-18E** T=52.5°C	**Well NEM-13E** T=66.6°C
H^+	pH: 8.50	pH: 8.50	pH: 7.70	pH: 7.16	pH: 7.29	pH: 7.65	pH: 6.45	pH: 8.30	pH: 7.87	pH: 7.45	pH: 7.60	pH: 8.51	pH: 8.33
Na^+	234.5	211.5	3034.7	2556.7	3000.0	3082.0	1947.0	209.2	402.5	844.1	1122.0	276.0	260.0
K^+	3.9	3.9	19.6	86.02	220.0	137.0	58.6	1.56	10.95	14.1	25.8	4.3	4.35
Ca^{2+}	3.2	3.6	601.2	540.28	614.83	618.0	356.7	5.61	23.6	400.8	312.6	7.21	6.41
Mg^{2+}	0.5	2.4	14.6	16.54	7.77	4.86	21.9	0.97	8.75	11.7	31.13	0.97	0.97
SiO_2	36.0	33.0	70.0	55.0	57.8	75.0	26.5	28.0	17.0	24.0	29.0	14.0	40.0
CO_3^{2-}	7.2	7.2	0.0	0.0	0.0	0.0	0.0	0.0	0.0	0.0	0.0	7.2	--
HCO_3^-	216.0	225.8	42.7	59.17	35.38	41.1	99.4	231.8	356.2	59.8	189.0	202.5	220.8
SO_4^{2-}	36.0	33.6	336.2	363.0	550.0	412.0	354.0	33.62	153.7	269.0	216.6	38.68	31.69
Cl^-	212.7	177.3	5566.6	4716.0	5584.95	5631.0	3439.0	180.8	368.8	1829.0	2092.2	244.6	225.2

Table E: Chemical analyses of the Aristino-Alexandroupolis geothermal waters (concentrations in mg/l) along with their temperatures (Kolios, 2001; Kolios et al., 2005; Poutoukis and Dotsika, 1988)

Ions	**Well AA-1E** T=80.0°C	**Well AA-1P** T=51.8°C	**Well AA-2E** T=30.5°C	**Well AA-3E** T=87.0°C	**Well AA-3P** T=89.0°C	**Well AA-4E** T=60.1°C	**Well AA-4P[1]** T=64.0°C	**Well AA-4P[2]**
H^+	pH: 7.44	pH: 7.72	pH: 7.27	pH: 7.89	pH: 7.58	pH: 7.72	pH: 7.91	pH: 8.11
Na^+	2000.0	2760.0	2600.0	3700.0	3400.0	2950.0	3300.0	3200.0
K^+	100.0	100.0	100.0	57.0	104.0	23.0	30.0	152.0
Ca^{2+}	340.7	521.04	472.15	353.5	517.03	328.65	391.68	529.06
Mg^{2+}	24.3	34.2	22.85	29.16	12.15	9.72	14.58	24.30
SiO_2	64.2	49.2	14.98	40.65	23.54	25.2	28.3	47.1
CO_3^{2-}	0.0	0.0	0.0	0.0	0.0	0.0	0.0	0.0
HCO_3^-	124.4	170.8	306.22	870.6	84.18	103.7	69.54	219.6
SO_4^{2-}	235.5	712.5	675.0	510.0	750.0	665.0	710.0	685.0
Cl^-	4255.2	5283.5	4982.13	5095.6	5665.9	4609.8	5212.62	5425.38

Ions	**Well AA-5P** T=32.5°C	**Well EB-1** T=42.5°C	**Well EB-3** T=92.5°C	**Well KO-1** T=82.5°	**Well AA-E (NE of Aristino)** T=76.5°C	**Traianoupolis Spring** T=51.0°C
H^+	pH: 7.95	pH: 7.78	pH: 7.04	pH: 6.61	pH: 7.80	pH: 7.00
Na^+	2500.0	1040.0	3080.0	2780.0	2976.8	2712.8
K^+	100.0	19.0	148.0	138.0	163.5	156.41
Ca^{2+}	334.27	95.0	561.0	325.0	636.6	541.0
Mg^{2+}	10.21	10.0	21.38	5.0	16.8	17.01
SiO_2	27.6	34.0	85.0	85.0	84.7	41.8
CO_3^{2-}	0.0	0.0	0.0	0.0	0.0	0.0
HCO_3^-	211.06	441.0	216.0	115.0	109.8	186.71
SO_4^{2-}	625.0	1500.0	800.0	725.0	528.6	561.97
Cl^-	3836.77	145.0	4960.0	4610.0	5571.5	4608.89